follows from

$$\lim_{\lambda_0,\lambda_2\to 0}(\partial \ln Z/\partial\lambda_2)=N\sum_i\langle x_j m_j\rangle=Ncz\langle m_1\rangle. \quad (6)$$

Thus, λ_2 was introduced to simplify the computation of $\langle m_1\rangle$. We note also that, for $h_j=n_j$,

$$\frac{1}{Nzc}\lim_{\lambda_0,\lambda_2\to 0}\frac{\partial \ln Z}{\partial\lambda_1}=\frac{1}{zc}\sum_i\langle x_j n_j m_j\rangle=\langle n_1 m_1\rangle. \quad (7)$$

The first-shell magnetic moment cannot be determined from (7) unless n_1 and m_1 are uncorrelated, i.e., unless

$$\langle n_1 m_1\rangle=\langle n_1\rangle\langle m_1\rangle. \quad (8)$$

Since, however, the internal field on the ith atom is proportional to n_i, the random variables n_i and m_i are correlated except in the case $c=0$ or 1. This correlation is neglected in reference 3 and invalidates the results therein. We now proceed to show that the correct result is independent of the concentration fluctuations in the second shell.

Using (3)–(6) we find, for small λ_1 (near the Curie temperature),

$$\begin{aligned}\langle m_0\rangle&=\tfrac{1}{3}S^2\lambda_1 zc\,\mathfrak{L}\langle h\rangle,\\ \langle m_1\rangle&=\tfrac{1}{3}S^2\lambda_1[1+\mathfrak{L}^2c^2(z-1)]\langle h\rangle.\end{aligned} \quad (9)$$

By the usual procedure of equating $\langle m_0\rangle$ and $\langle m_1\rangle$, we arrive at Smart's result,

$$\mathfrak{L}(2JS^2/kT_c)=1/c(z-1). \quad (10)$$

We remark, incidentally, that only the mean and variance of the distribution of magnetic atoms in the first shell enters into the calculation, the results being independent of higher moments of the distribution. In a similar way, only the mean, or first moment of the distribution of molecular fields (which may be thought of as arising from magnetic atoms in the second shell), enters when the molecular field is allowed to fluctuate. We conclude that proper account of the fluctuations in the second shell within the BPW scheme would probably involve enlarging the BPW cluster.

ACKNOWLEDGMENT

The author would like to thank T. A. Kaplan for several informative discussions.

PHYSICAL REVIEW VOLUME 128, NUMBER 5 DECEMBER 1, 1962

Nuclear Magnetic Resonance in the Demagnetized State

A. G. ANDERSON
IBM Research Laboratory, San Jose, California

AND

S. R. HARTMANN*
Physics Department, University of California, Berkeley, California

(Received May 17, 1962)

A discussion is given of experimental results and theoretical considerations which apply in the case of complete adiabatic demagnetization in the rotating frame (ADRF) for nuclear spin systems in solids. Although the net magnetization in this state is zero, both continuous wave and pulse signals are predicted and readily observed at the normal resonance frequency. These signals appear to be much like the derivative of the signals observed in the normal nuclear magnetic resonance (NMR) cases with amplitudes comparable to normal NMR signal amplitudes and they persist for times comparable with T_1 at high fields even when the line is purely homogeneously broadened. A simple heuristic theory is used to calculate, after ADRF, the shape of the free-induction decay and the form of the absorption at $\omega\approx 0$, Ω, and 2Ω, where Ω is the resonance frequency of the spin system. The density matrix method is then used to calculate line shapes and free-induction decay signals which are found to be in agreement with experiment and the heuristic model calculation. The concept of spin temperature is used to calculate the effect of applying an rf field to produce a line asymmetry in a homogeneously broadened system. It is also shown that, in general, the free induction decay signal is not the Fourier transform of the line shape and homogeneously broadened lines do not saturate uniformly. In addition, it is found experimentally that ADRF is reversible, spin systems are coupled, spectra at low frequency and double the resonance frequency are observed, and spin-system relaxation times vary rapidly with field at low dc fields but are of order of T_1 at high fields.

I. INTRODUCTION

THE technique of adiabatic demagnetization has been used in many experiments,[1] the most common one being that in which a lattice containing magnetic spins is cooled to very low temperatures. After adiabatic demagnetization the previous large applied dc field is replaced by the random local internal dipole or exchange fields due to neighboring magnetic

* Work supported in part by Office of Naval Research and National Science Foundation.

[1] See, for example, C. B. Garrett, *Magnetic Cooling* (Harvard University Press, Cambridge, Massachusetts, 1954); A. Abragam and W. G. Proctor, Phys. Rev. **109**, 1441 (1958); L. C. Hebel and C. P. Slichter, *ibid.* **107**, 901 (1957).

spins and the net magnetization is zero. This state of the spin system does not lend itself to investigation by direct nuclear magnetic resonance (NMR) techniques since there is no large dc field available to define a direction and force the spins to precess at frequencies which are readily observable. However, by using techniques similar to those of Slichter and Holton[2] it is possible to perform an adiabatic demagnetization experiment in a large constant dc field so that the final state is much like that described above with the significant difference that a large dc field is present in which NMR experiments can be performed.

In order to explain observed results at high rf power in homogeneously broadened nuclear resonance systems, it was necessary for Redfield[3] to consider serious modifications of the then existing NMR theory. The pertinent point for the discussions there was the assumption that, upon transforming the spin system Hamiltonian to the frame rotating at the frequency of the applied rf, the density matrix of the spin system in this frame was to be described by a Boltzmann distribution characterized by the secular parts of the *transformed* Hamiltonian. At high rf fields, this was equivalent to assuming that the magnetization is aligned along the direction of the effective field in the rotating frame. Redfield gave arguments for the applicability of this assumption for rf H_1 fields which are much higher than (or of the order of), the rf fields necessary for saturation.

More recently, Slichter and Holton[2] and Goldburg[4] have verified the applicability of this concept down to H_1 fields of considerably less than the internal fields. We report here the treatment of the case where H_1 is reduced to zero.

An intuitive feeling for much of what follows can be obtained by considering the case of an *inhomogeneously* broadened line under conditions of long spin-lattice relaxation time, T_1, and partial fast passage. Here the dc field sweep, with rf (H_1) applied at constant frequency, is started far from the line and swept to the line center; at this point the dc sweep is stopped and the large rf H_1 is slowly lowered to zero. As $H_1 \rightarrow 0$ the effective field in the rotating frame tilts upward for higher frequency spins and downward for lower frequency spins. The result is a resonance line which on one side absorbs and on the other side emits energy when a small rf field is used to measure the absorption line shape. The spin system after adiabatic demagnetization in the rotating frame (ADRF) is left with zero net magnetization and a total energy of order $\delta H/H_0$ times its original energy (where δH is the inhomogeneous linewidth), but the line can readily be seen by normal NMR, continuous wave (cw), or pulse techniques.

Now, although the homogeneously broadened spin systems cannot be as simply described as the case above, many of the experiments associated with ADRF can be visualized with this model and the technique for producing the ADRF state is much the same. To illustrate the type of results found (Fig. 1), the experimental curves indicate derivative type lines after ADRF, as compared with the normal NMR signals. It is also found that application of a 90° pulse following

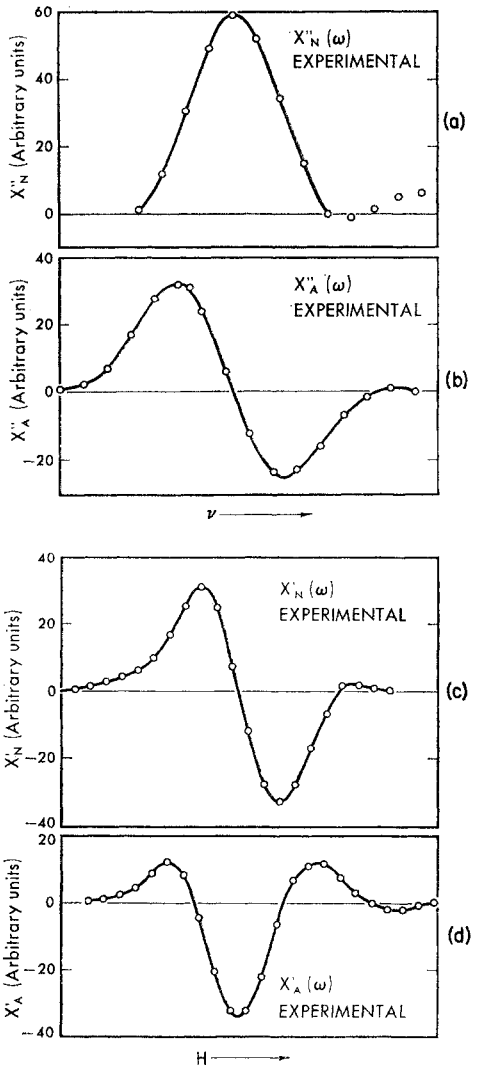

FIG. 1. Observed resonance lines in the normal and in the demagnetized cases. The sample used was Li^7 in a lithium metal dispersion, a case where one should expect predominant homogeneous line broadening. The center frequency in all cases was 1.1 Mc/sec, the same amplitude scale is used throughout, and the lines are: (a) The absorption mode line as seen on a sweep through resonance; see Fig. 3(b). The solid line is a fit of the experimental data in each of these figures. (The additional bump on the right is believed to be an extraneous experimental effect.) (b) The absorption mode line as seen on a sweep through resonance for the case of ADRF; see Fig. 3(e). The case shown has a *negative* temperature in the dipole-dipole system, as explained later in the text. (c) The dispersion mode line for the normal case. (d) The dispersion mode line as seen on a passage through resonance after ADRF.

[2] C. P. Slichter and W. C. Holton, Phys. Rev. **122**, 1701 (1961).
[3] A. G. Redfield, Phys. Rev. **98**, 1787 (1955).
[4] W. I. Goldburg, Phys. Rev. **122**, 831 (1961).

ADRF produces an output signal which is initially zero, but which rises to a maximum in a time of order T_2 and which then falls off to zero. These two results would be the same with either homogeneous or inhomogeneous line broadening. In other respects, however, the homogeneously broadened ADRF line has spectra and relaxation characteristics which are not found in the other case.

On the basis of past theory[5] and experiment[6] it can be seen that Zeeman and dipole-dipole contributions to the total energy of a spin system can have a decidedly nonequilibrium ratio when T_1 is long. That this can be so follows from the fact that, although matrix elements exist to couple these energy terms, the transitions which bring dipole-dipole and Zeeman energies into balance with one another are strongly inhibited at high dc fields because of requirements for over-all conservation of energy. By the arguments of Kronig and Boukamp,[5] conservation of energy requires that the local field be instantaneously equal to the applied dc field; since this is a rare event when the dc field is large, the time for establishment of internal equilibrium can be very long. In the ADRF state the Zeeman energy must be zero; the dipole-dipole energy is considerably different from zero, however, since, if the process is truly adiabatic, the order of the system (which before ADRF resided mainly in the Zeeman alignment with respect to the external dc field) must now be in spin alignment in dipole-dipole fields. This dipole-dipole alignment will persist for times of order T_1 if the dc field is high. If the field is reduced to a value of order $\langle \Delta H^2 \rangle^{1/2}$, then the ADRF state will decay rapidly as Zeeman and dipole-dipole energies come rapidly into equilibrium.

An additional interesting characteristic of the ADRF state occurs in homogeneously broadened systems with several spin species. In this case one can expect that, although the various spin species may be completely independent in the normal NMR case, the spin systems will readily couple in the ADRF state. To see this, assume that order exists in spin system 1 by alignment in dipole-dipole fields; then part of this alignment can be transferred to system 2 by multiple spin flips between systems 1 and 2 which, over all, conserve energy. Redfield[3] discussed a similar case of coupling when $H_1 \neq 0$.

Experimental and theoretical analysis of the considerations outlined above will be treated in the following discussions.

II. QUALITATIVE TREATMENT

In this section an admittedly crude theory is used to derive the line shape before and after ADRF. It is hoped that the lack of rigor is at least compensated for by the added insight obtained in considering the following heuristic arguments. Our considerations will apply to a line which is both homogeneously and inhomogeneously broadened.

The behavior of a set of nuclear spins in a large dc magnetic field when acted on by small applied rf magnetic field can be calculated if $\rho(\omega)$, the net spin polarization per unit angular frequency along the dc field, is known. If $g_{\pm}(\omega)$ is defined as the nuclear spin density per unit angular frequency aligned (along against) the dc magnetic field, then

$$g_+(\omega)=\frac{g(\omega)e^{\Delta E/2kT}}{e^{\Delta E/2kT}+e^{-\Delta E/2kT}}\approx(\tfrac{1}{2})g(\omega)e^{\Delta E/2kT}, \quad (1)$$

$$g_-(\omega)=\frac{g(\omega)e^{-\Delta E/2kT}}{e^{\Delta E/2kT}+e^{-\Delta E/2kT}}\approx(\tfrac{1}{2})g(\omega)e^{-\Delta E/2kT}, \quad (2)$$

and

$$\rho(\omega)\approx\tfrac{1}{2}\,g(\omega)(\Delta E/kT), \quad (3)$$

where $\exp(-\Delta E/kT)$ is the usual Boltzmann factor. $g(\omega)$ represents the frequency distribution of the individual nuclear spins and is normalized to unity, i.e.,

$$\int_0^\infty g(\omega)d\omega=1. \quad (4)$$

If an rf magnetic field is applied near Ω, where $\Omega=\gamma H_0$, then the energy absorbed will be given by

$$A(\omega)=K\omega\rho(\omega), \quad (5)$$

or

$$A(\omega)=K\omega(\Delta E/2kT)g(\omega), \quad (6)$$

where K is a constant determined by the strength of the interaction. In the normal resonance experiment the whole spin system is in thermal equilibrium with the lattice so that

$$\Delta E=\hbar\omega,$$

and therefore

$$A_N(\omega)=K\hbar(\omega^2/2kT)g(\omega). \quad (7)$$

The subscript N signifies the normal result. Using the standard expression[7] for $A(\omega)$ given by

$$A(\omega)=\pi\omega^2\chi_0H_1^2g(\omega), \quad (8)$$

we can evaluate the constant K:

$$K=2\pi\,\mathrm{Tr}M_x^2H_1^2/h\alpha, \quad (9)$$

where $\alpha=\mathrm{Tr}1$.

If we now perform an adiabatic demagnetization in the rotating frame (ADRF), each nucleus which was originally polarized in the applied dc magnetic field is now polarized in its own local field. In this way, nuclei in the center of the line become completely depolarized, while nuclei on the high-field side of the line tend to

[5] R. Kronig and C. J. Bouwkamp, Physica **5**, 521 (1938).

[6] P. R. Locher and J. C. Verstelle, *Proceedings of Seventh International Conference on Low-Temperature Physics* (University of Toronto Press, Toronto, 1960), p. 56.

[7] A. Abragam, *The Principles of Nuclear Magnetism* (Clarendon Press, Oxford, 1961); L. S. Brown, IBM J. Research Develop. **6**, 338 (1962); A. Wright, Phys. Rev. **76**, 1826 (1949).

remain polarized in the direction of the dc magnetic field and nuclei on the low-field side of the line are inverted. We have essentially shifted the effective zero field from $\omega=0$ to $\omega=\Omega$. In this way ΔE is given by $\hbar(\omega-\Omega)$, and T is the effective spin temperature of the nuclear spin system T_S. Using the subscript D to denote the fact that after ADRF the energy of the system is due solely to dipole-dipole interactions, we can substitute for ΔE into Eq. (6) to obtain[8]

$$A_D(\omega)=K\hbar[(\omega-\Omega)/2kT_S]\omega g(\omega). \tag{10}$$

As in other adiabatic demagnetization experiments,[1] the spin temperature after ADRF is related to the lattice temperature by the relation

$$T_S=(\omega_L/\Omega)T, \tag{11}$$

where

$$\omega_L=\gamma H_L, \tag{12}$$

and H_L is an effective local field (to be derived later). Writing $A_D(\omega)$ in terms of T, we find

$$A_D(\omega)=[(\omega-\Omega)/\omega_L]K\hbar(\omega\Omega/2kT)g(\omega). \tag{13}$$

For $\omega-\Omega\cong\omega_L$ then, $g(\omega)\approx g(\Omega)$ and the absorption signal from a spin system after ADRF is comparable in magnitude to that in the normal case (see Fig. 1).

The case in which all the energy is in the Zeeman system is obtained by setting $T_S=T$ and taking the difference of Eqs. (7) and (10) to yield

$$A_Z(\omega)=K\hbar(\omega\Omega/2kT)g(\omega), \tag{14}$$

where the subscript Z indicates that the energy is only in the Zeeman terms. Equation (14) could have been obtained by stating that an adequate description for $\rho_Z(\omega)$ is obtained by setting

$$\Delta E=\hbar\Omega. \tag{15}$$

The above results for $A_N(\omega)$, $A_D(\omega)$, and $A_Z(\omega)$ will be shown in Sec. III to be identical with results obtained using a rigorous technique.

Absorption at $\omega\approx0$ and $\omega\approx2\Omega$

We now calculate the absorption at $\omega\approx0$ and $\omega\approx2\Omega$. At $\omega\approx0$ energy can be absorbed from an rf field by a mutual spin-flip process $\uparrow\downarrow\rightarrow\downarrow\uparrow$ in which the frequency separation of the two spins is just ω. We write the absorption as

$$A^{(0)}(\omega)=K_0\omega\int_0^\infty[g_-(\omega')g_+(\omega+\omega')-g_+(\omega')g_-(\omega+\omega')]d\omega', \tag{16}$$

where K_0 depends on the strength of the interaction with the rf field. The quantity $g_-(\omega')g_+(\omega+\omega')$ is proportional to the probability of exciting a $\uparrow\downarrow\rightarrow\downarrow\uparrow$ transition, while $g_+(\omega')g_-(\omega+\omega')$ is the probability of exciting the reverse transition. The above expression is integrated over ω' to obtain the absorption from spins anywhere in the resonance line. Using Eqs. (2) and (3), $A^{(0)}(\omega)$ becomes

$$A^{(0)}(\omega)=\frac{K_0\omega}{4kT}\int_0^\infty g(\omega')g(\omega+\omega')\times[\Delta E(\omega+\omega')-\Delta E(\omega')]d\omega'. \tag{17}$$

In the normal case $\Delta E(\omega)=\hbar\omega$, we obtain

$$A_N^{(0)}(\omega)=\frac{K_0\hbar\omega^2}{4kT}\int_0^\infty g(\omega')g(\omega+\omega')d\omega'. \tag{18}$$

The absorption in this case has been calculated by Wright and by Brown[7] who obtained

$$A^{(0)}(\omega)=\pi\omega^2\chi_0H_1^2g_0(\omega), \tag{19}$$

where

$$\int_{-\infty}^\infty g_0(\omega)d\omega=\langle\Delta\omega_0^2\rangle/\Omega^2, \tag{20}$$

where $\langle\Delta\omega_0^2\rangle$ is the second moment of the line.

The constant K_0 is determined by requiring that $(1/\omega)^2$ times the integrated absorptions obtained from Eqs. (18) and (19) are equal and assuming a Gaussian form for $g(\omega)$,

$$g(\omega)=[T_2/(2\pi)^{1/2}]\exp[-(\omega-\Omega)^2T_2^2/2], \tag{21}$$

where $T_2=1/\langle\Delta\omega_0^2\rangle^{1/2}$. Function $g(\omega)$ is normalized to unity. We then obtain

$$K_0=4\pi\frac{\mathrm{Tr}M_x^2}{\alpha\hbar}\frac{\langle\Delta\omega_0^2\rangle H_1^2}{\Omega^2} \tag{22}$$

to yield

$$A_N^{(0)}(\omega)=\frac{\pi\langle\Delta\omega_0^2\rangle}{2\Omega^2}H_1^2\frac{\mathrm{Tr}M_x^2}{\alpha kT}\omega^2\frac{T_2}{\pi^{1/2}}\exp(-\omega^2T_2^2/4). \tag{23}$$

Defining the normalized function

$$G_0(\omega)=(T_2/2\pi^{1/2})\exp(-\omega^2T_2^2/4); \tag{24}$$

then

$$A_N^{(0)}(\omega)=\frac{\pi\langle\Delta\omega_0^2\rangle}{\Omega^2}\frac{\mathrm{Tr}M_x^2}{\alpha kT}\omega^2G_0(\omega)H_1^2. \tag{25}$$

In the case where all the energy is in the Zeeman term, then, by Eq. (17),

$$A_Z^{(0)}(\omega)=0. \tag{26}$$

This means that, in this model, no absorption is expected at $\omega\approx0$ if only Zeeman energy is considered. The absorption after ADRF is then identical to Eq. (25) with T replaced by T_S. Using Eq. (11), we obtain

$$A_D^{(0)}(\omega)=(\Omega/\omega_L)A_N^{(0)}(\omega). \tag{27a}$$

In the case where the spin system is polarized at $\omega=\Omega_\rho$

[8] A similar expression for $A_D(\omega)$ has been independently obtained by A. Abragam (private communication).

and demagnetized at $\omega=\Omega$, we obtain

$$A_D^{(0)}(\omega)=(\Omega_\rho/\omega_L)A_N^{(0)}(\omega). \tag{27b}$$

The zero-frequency line is therefore enhanced by a factor Ω/ω_L following adiabatic demagnetization.

The practical sensitivity is even greater than this since in the normal state, at high dc fields, the absorption at $\omega\approx 0$ would only increase the energy in the dipole-dipole system and reduce the slight asymmetry in line shape at $\omega\approx\Omega$ without affecting its magnitude. It is only after ADRF when the line shape is due solely to dipole-dipole interactions that absorption at $\omega\approx 0$ would affect the magnitude of the central resonance to first order.

The absorption at $\omega=2\Omega$ is obtained by mutual spin-flip processes of the form $\uparrow\uparrow\leftrightarrow\downarrow\downarrow$. The absorption is given by

$$A^{(2)}(\omega)=K_2\omega\int_0^\infty[g_+(\tfrac{1}{2}\omega+\omega')g_+(\tfrac{1}{2}\omega-\omega') -g_-(\tfrac{1}{2}\omega+\omega')g_-(\tfrac{1}{2}\omega-\omega')]d\omega'. \tag{28}$$

By the methods used to obtain $A^{(0)}$, and with[7]

$$A_N^{(2)}(\omega)=\pi\omega^2\chi_0H_1^2g_2(\omega), \tag{29}$$

$$\int_0^\infty g_2(\omega)d\omega=\frac{2}{3}\frac{\langle\Delta\omega_0^2\rangle}{\Omega^2}, \tag{30}$$

the assumption of a Gaussian line shape, and with a function, G_2, defined by

$$G_2(\omega)=(T_2/2\pi^{1/2})\exp[-(\omega-2\Omega)^2T_2^2/4], \tag{31}$$

one obtains

$$A_N^{(2)}(\omega)=\frac{2\pi\langle\Delta\omega_0^2\rangle}{3\Omega^2}\frac{\mathrm{Tr}M_x^2}{\alpha kT}\omega^2G_2(\omega)H_1^2. \tag{32}$$

In like manner,

$$A_Z^{(2)}(\omega)=(\Omega/\omega)A_N^{(2)}(\omega), \tag{33}$$

and

$$A_D^{(2)}(\omega)=\frac{(\omega-2\omega)}{\omega}\frac{T}{T_S}A_N^{(2)}(\omega), \tag{34}$$

and, using Eq. (11),

$$A_D^{(2)}(\omega)=\frac{\Omega}{\omega_L}\frac{(\omega-2\Omega)}{\omega}A_N^{(2)}(\omega). \tag{35}$$

Since $G(2\Omega+1/T_2)\approx G(2\Omega)$ and $\langle\Delta\omega_0^2\rangle/\omega_L^2\approx 1$,

$$A_D^{(2)}(2\Omega)\approx A_Z^{(2)}(2\Omega). \tag{36}$$

In the determination of $A_D^{(2)}(\omega)$ it is necessary to irradiate at $\omega\approx 2\Omega$ and to then traverse the resonance line at $\omega=\Omega$ to determine the reduction in line amplitude. However, the energy absorbed by the nuclear spins does not all go into the dipole system; the larger part of the energy goes into the Zeeman system. The actual energy absorbed by the dipole system $A_D^{(2)*}(\omega)$ is given by expression (28) with the factor ω replaced by $(\omega-2\Omega)$. This comes about since each spin flip gives $\pm\hbar\Omega$ of energy to the Zeeman system so that mutual spin flips at $(\omega/2)+\omega'$ and $(\omega/2)-\omega'$ give up only $\pm\hbar(2\Omega-\omega)$ of energy to the dipole system. Using Eq. (35), we then obtain

$$A_D^{(2)*}(\omega)=\frac{\Omega}{\omega_L}\left(\frac{\omega-2\Omega}{\omega}\right)^2A_N^2(\omega). \tag{37a}$$

In the case where the system is polarized at $\omega=\Omega_\rho$, we obtain

$$A^{(2)*}(\omega,\Omega_\rho)=(\Omega_\rho/\Omega)A^{(2)*}(\omega). \tag{37b}$$

Comparing Eqs. (37b) and (27b), we note that the zero-frequency line is 3/2 more sensitive than the line at 2Ω, insofar as saturation of the dipole-dipole energy is concerned.

Free-Induction Decay Signal

We now calculate the form of the free-induction decay signal using the arguments above. If we apply a short, intense θ^0 rf pulse ($\theta=\omega_{rf}\tau$, where $\omega=\gamma H_{rf}$; H_{rf} is the component of the applied rf magnetic field circularly polarized in the same sense of rotation as the precessing nuclear spins; τ is the length of the pulse) at the frequency Ω, we expect to obtain a free-precession signal proportional to M, where

$$M=P\sin\theta\int_{-\infty}^{\infty}\rho(\omega)\exp(i\omega t)d\omega, \tag{38}$$

and

$$P=\mathrm{Tr}M_x^2/\gamma\hbar\alpha.$$

Using Eqs. (1), (2), and (3),

$$M_Z=\frac{P\hbar\Omega\sin\theta}{2kT}\int_{-\infty}^{\infty}g(\omega)\exp(i\omega t)d\omega, \tag{39}$$

and

$$M_D=\frac{P\hbar\sin\theta}{2kT_S}\int_{-\infty}^{\infty}(\omega-\Omega)g(\omega)\exp(i\omega t)d\omega. \tag{40}$$

These expressions can be rewritten as

$$M_Z=(P\hbar\Omega\sin\theta/2kT)G(t)\exp(i\Omega t), \tag{41}$$

and

$$M_D=i(P\hbar\sin\theta/2kT_S)[dG(t)/dt]\exp(i\Omega t), \tag{42}$$

where

$$G(t)=\int_{-\infty}^{\infty}g(\omega)\exp[i(\omega-\Omega)t]d\omega. \tag{43}$$

The quantity $G(t)$ describes the form of the free-induction decay envelope.

In the following discussion, we consider a solid with two magnetic species a and b. If the a system is demagnetized, then the net a spin magnetization in the sample is zero so that immediately after the rf pulse, the free-induction signal is zero. However, although the net a spin magnetization is zero before the rf pulse

is applied, in the region just above $\omega=\Omega$ there is a net magnetization directed along H_0 while just below $\omega=\Omega$ the spins are directed against H_0. After the rf pulse the vector sum of the magnetization from spins above and below $\omega=\Omega$ initially cancel, but then the spins above $\omega=\Omega$ precess faster than those below $\omega=\Omega$ and finally reinforce to yield a large nuclear signal.

As will be shown later, Eq. (42) is correct only when the line is inhomogeneously broadened. When this is not true the θ^0 rf pulse also tips the local field and this must be taken into consideration. For a Gaussian line Eq. (42) predicts

$$M_D(t)=\frac{M_0\sin\theta}{\langle\Delta\omega_L{}^2\rangle^{1/2}}[\langle\Delta\omega_{aa}{}^2\rangle + \langle\Delta\omega_{ab}{}^2\rangle]t\exp(-t^2/2T_2{}^2)\cos\Omega t, \quad (44)$$

where T_2 is the spin-spin relaxation time:

$$1/T_2{}^2=\langle\Delta\omega_{aa}{}^2\rangle+\langle\Delta\omega_{ab}{}^2\rangle=\gamma^2(\bar{\Delta}H)^2. \quad (45)$$

$\langle\Delta\omega_{aa}{}^2\rangle$ is the second moment[9] of A spins due to other A spins; $\langle\Delta\omega_{ab}{}^2\rangle$ is the second moment[9] of A spins due to B spins; $\langle\Delta\omega_L{}^2\rangle^{1/2}=\gamma H_L=\omega_L$; M_0 is the net excess magnetization of the A spins, i.e., $M_0=\mathrm{Tr}M_x{}^2\Omega/\gamma\alpha kT$.

It is now possible to correct Eq. (44) by multiplying $\langle\Delta\omega_{aa}{}^2\rangle$ by the factor $\cos\theta$ which would take into account the flipping of the local field at the a spins which are also being flipped. This gives us the expression

$$M_A(t)=\frac{M_0\sin\theta}{\langle\Delta\omega_L{}^2\rangle^{1/2}}[\langle\Delta\omega_{aa}{}^2\rangle\cos\theta + \langle\Delta\omega_{ab}{}^2\rangle]t\exp(-t^2/2T_2{}^2)\cos\Omega t, \quad (46)$$

which is, in fact, in good agreement with experiment.

This treatment, although qualitative, explains the experimental results obtained for the spectra around the Larmor frequency exactly and further describes the absorption at $\omega\simeq 2\Omega$ in a qualitative manner.

III. QUANTITATIVE TREATMENT

In this section the properties of a spin system after ADRF are calculated more exactly. It is found that in those cases where it was possible to calculate similar quantities, the results agree with those of the previous section. The two sections do not overlap completely, however; in that section the line shape at $\omega\approx 0$ and $\omega\approx 2\Omega$ was obtained, while in this section consideration is given to mixing of the Zeeman and dipole systems due to rf irradiation.

We first consider the process of ADRF. There are two techniques for carrying out ADRF: One can either perform a fast passage to the center of the line with a low intensity rf magnetic field or one can "spin lock"[10] the magnetization with a strong rf magnetic field and then proceed to turn off the rf field adiabatically. The second technique will be considered first.

Consider a nuclear spin system containing two different nuclear species labeled by a and b. The Hamiltonian of the system is given by

$$\mathcal{H}=\mathcal{H}_0+\mathcal{H}_1+\mathcal{H}_2+\mathcal{H}_3, \quad (47)$$

where

$$\mathcal{H}_0=\hbar\Omega_a\textstyle\sum_n I_{zn}{}^a+\hbar\Omega_b\sum_n I_{zn}{}^b, \quad (48)$$

$$\mathcal{H}_1=2\hbar\omega_1\textstyle\sum_n I_{xn}{}^a\cos\omega_a t, \quad (49)$$

$$\mathcal{H}_2=\sum_{ij}[A_{aij}\mathbf{I}_i{}^a\cdot\mathbf{I}_j{}^a+B_{aij}I_{zi}{}^aI_{zj}{}^a+A_{bij}\mathbf{I}_i{}^b\cdot\mathbf{I}_j{}^b + B_{bij}I_{zi}{}^bI_{zj}{}^b+C_{ij}I_{zi}{}^aI_{zj}{}^b], \quad (50)$$

where

$$A_{ij}=J_{ij}+\frac{\gamma^2\hbar}{r_{ij}{}^3}(\tfrac{3}{2}\cos^2\theta_{ij}-\tfrac{1}{2}), \quad (51)$$

$$B_{ij}=\frac{3\gamma^2\hbar}{r_{ij}{}^3}(\tfrac{3}{2}\cos^2\theta_{ij}-\tfrac{1}{2}), \quad (52)$$

$$C_{ij}=\frac{\gamma^a\gamma^b\hbar}{r_{ij}{}^3}(1-3\cos^2\theta_{ij})+J_{ij}{}^{ab}, \quad (53)$$

where J_{ij} is due to exchange-type interactions,[11] r_{ij} is the distance between the ith and jth atom; θ_{ij} is the angle between $\mathbf{r}_{ij}$ and $\mathbf{H}_0$. The Hamiltonian $\mathcal{H}_2$ takes into account spin-spin interactions due to dipole-dipole and effective exchange interactions. All the nonsecular dipole-dipole terms are contained in $\mathcal{H}_3$. Since we will only consider experiments at high dc fields, this term will not be considered further.

The process of ADRF is carried out as follows: (1) Apply an intense 90° rf pulse to the a spins at the frequency $\omega=\Omega_a$; (2) immediately after the 90° rf pulse, shift the phase of the rf magnetic field by 90° and then slowly turn off the rf magnetic field.

All quantities of interest will be calculated using the density matrix[12] ρ which satisfies the equation

$$d\rho/dt=(-i/\hbar)[\mathcal{H},\rho], \quad (54)$$

and which has the property that the expectation value of any operator Q is given by

$$\langle Q\rangle=\mathrm{Tr}(\rho Q). \quad (55)$$

If the nuclear spin system is in thermal equilibrium with the lattice, then[12]

$$\rho=[\exp(-\mathcal{H}/kT)/\alpha], \quad (56)$$

where

$$\alpha=\mathrm{Tr}\exp(-\mathcal{H}/kT).$$

Before the rf pulse is applied, assume that the spin

[9] J. H. Van Vleck, Phys. Rev. **74**, 1168 (1948).
[10] I. Solomon, Compt. rend. **248**, 92 (1950); S. R. Hartmann and E. L. Hahn, Bull. Am. Phys. Soc. **5**, 498 (1960).
[11] H. A. Ruderman and C. Kittel, Phys. Rev. **96**, 99 (1954).
[12] R. C. Tolman, *The Principles of Statistical Mechanics* (Oxford University Press, New York, 1938); U. Fano, Revs. Modern Phys. **29**, 74 (1957).

system has come into thermal equilibrium with the lattice, and since $\mathcal{H}_0$ is large compared with $\mathcal{H}_{\text{int}}$, make the approximation

$$\rho=[\exp(-\mathcal{H}_0/kT)/\alpha]. \tag{57}$$

Making the transformation

$$\rho=\exp[(-i/\hbar)\mathcal{H}_0t]\rho^*\exp[(i/\hbar)\mathcal{H}_0t], \tag{58}$$

then $\rho_0^*=\rho_0$ and ρ^* satisfies the equation

$$d\rho^*/dt=(-i/\hbar)[\mathcal{H}^*,\rho^*], \tag{59}$$

where $\mathcal{H}^*=\mathcal{H}_1^*+\mathcal{H}_2^*$, $\mathcal{H}_1^*=\omega_1\hbar\sum_n I_{xn}^a$, and $\mathcal{H}_2^*=\mathcal{H}_2$. At $t=0$ an intense rf pulse of magnitude ω_1 is turned on. When the 90° pulse condition has been reached the density matrix will be of the form [13]

$$\rho_{90^\circ}^*=\exp(-\Omega_\alpha\hbar\textstyle\sum_n I_{yn}^a/kT)/\alpha, \tag{60}$$

at which time the phase of the rf pulse is shifted by 90° so that $\mathcal{H}_1^*$ is now given by

$$\mathcal{H}_1^*=\omega_1\hbar\textstyle\sum_n I_{yn}^a. \tag{61}$$

The I_z^b term has been dropped since the Zeeman energy in the b system is not affected by the ADRF experiment applied to the a system. Using the value of $\mathcal{H}_1^*$ given by Eq. (61), it is found that

$$[\rho_{90^\circ}^*,\mathcal{H}_1^*+\mathcal{H}_2]=[\rho_{90^\circ}^*,\mathcal{H}_2], \tag{62}$$

so that there is a slight change in ρ^* due to the dipole-dipole interactions, while the spins are virtually not affected by the presence of the intense rf field represented by $\mathcal{H}_1^*$. We now assume, following Redfield,[3] that the a spins can be described by a spin temperature so that ρ^* is given by

$$\rho^*=\exp[(\mathcal{H}_1^*+\mathcal{H}_2)/kT_S]/\alpha, \tag{63}$$

and the spin temperature is virtually unchanged from its value in Eq. (60) since $\mathcal{H}_1^*\gg\mathcal{H}_2$. Since the rf pulse was intense, $\mathrm{Tr}(\mathcal{H}_1^*)^2\gg\mathrm{Tr}(\mathcal{H}_2^*)^2$ and therefore the substitution of

$$T_S=T(H_1/H_0) \tag{64}$$

into Eq. (63) approximates Eq. (60). The new expression for ρ^*, Eq. (63), commutes with $\mathcal{H}^*$, and consequently it will not change with time as long as $\mathcal{H}^*$ is not varied. The ADRF is now accomplished by turning off ω_1 slowly enough so that the total entropy remains constant. As ω_1 is decreased, the form of ρ^* given by Eq. (63) will remain constant, but T_S will vary according to the formula

$$T_S=T[(H_1^2+H_L{}^{a2})/(H_0^2+H_L{}^{a2})]^{1/2}, \tag{65}$$

where

$$H_L{}^a=[\mathrm{Tr}\mathcal{H}_2^2/\mathrm{Tr}M_z{}^{a2}]^{1/2}. \tag{66}$$

It should be pointed out that $H_L{}^a$ is a fictitious field which only approximates the local field $(1/\gamma)\langle\Delta\omega_0^2\rangle^{1/2}$ for a solid containing a single spin system with negligible exchange and is much larger in cases where other abundant spin systems are present. This expression is obtained by following the procedure of Abragam and Proctor[1] in the analogous experiment of the ordinary adiabatic demagnetization obtained by turning off the large dc magnetic field. The expression for $H_L{}^a$ differs from Abragam and Proctor's result in that the trace of only the secular interaction Hamiltonian is used in obtaining $H_L{}^a$ instead of including the complete interaction Hamiltonian.

Using the condition $H_0\gg H_L{}^a$, we find that at $H_1=0$

$$T_S{}^0=T(H_L{}^a/H_0), \tag{67}$$

and the density matrix after ADRF is given by

$$\rho_0^*=\exp(-\mathcal{H}_2/kT_S{}^0)/\alpha. \tag{68}$$

In order to regain the magnetization after ADRF, it is necessary to reverse the process described above. By slowly applying an rf magnetic field at the frequency Ω_α, the magnetization can be restored. It is interesting to point out that one could adiabatically magnetize at the frequency Ω_b, and in this way one should be able to lower the entropy of the b spins by an amount equal to the initial entropy of the a spins, less that entropy of the a spins associated with complete disorder. Since the spin temperature, T_f, the b spins would attain after adiabatic magnetization is given by [using Eq. (65)]

$$T_f=T_S(H_0/H_L{}^b), \tag{69}$$

we obtain the result that

$$T_f=T(H_L{}^a/H_L{}^b), \tag{70}$$

suggesting a possible means of dynamic polarization. *Note added in proof.* This method of transfer of entropy from system a to system b has been demonstrated by one of us (SRH) in NaCl.

The attainment of ADRF by fast passage to the center-of-resonance line yields the same result as obtained above. The technique is different, however, and it is interesting to consider it in some detail. Since the rf field is applied at the frequency ω, where $(\omega-\Omega)/\langle\Delta\omega_0^2\rangle^{1/2}\gg1$, we are led to make the initial transformation of

$$\rho=\exp(-i\omega\textstyle\sum_n I_{zn}^a)\rho^*\exp(i\omega\sum_n I_{zn}^a), \tag{71}$$

where ρ^* satisfies Eq. (59) and $\mathcal{H}^*$ is now given by

$$\mathcal{H}^*=\hbar(\Omega_a-\omega)\textstyle\sum_n I_{zn}^a+\hbar\Omega_b\sum_n I_{zn}^b+\mathcal{H}_2+\hbar\omega_1\sum_n I_{xn}^a. \tag{72}$$

The applied rf field is small, meaning

$$\mathrm{Tr}\mathcal{H}_2^2\gg\mathrm{Tr}(\hbar\omega_1\textstyle\sum_n I_{xn}^a)^2. \tag{73}$$

Equation (72) should be compared with the Hamiltonian for a set of spins in a large dc field which is just Eq. (47) without the rf field term. The usual adiabatic demagnetization experiment is performed by slowly

[13] I. I. Lowe and R. E. Norberg, Phys. Rev. **107**, 46 (1957).

decreasing the magnetic field H_0 so that order is transferred from the $\mathcal{H}_0$ system to the $\mathcal{H}_2+\mathcal{H}_3$ system because of the coupling provided by $\mathcal{H}_3$. The speed with which one can successfully adiabatically demagnetize depends on the magnitude of $\mathcal{H}_3$; the stronger the coupling, the faster one can reduce the dc field and still conserve entropy. In the case of ADRF the effective magnetic field for the a spins is decreased as $\omega \rightarrow \Omega_a$, so that energy flows from the $\hbar(\Omega_a-\omega)\sum_n I_{zn}{}^a$ system to the $\mathcal{H}_2$ system because of the coupling now provided by the term $\hbar\omega_1 \sum_n I_{xn}{}^a$. The rf term now takes the place of the nonsecular term in $\mathcal{H}_3$. In principle, then, one could adiabatically demagnetize with an arbitrarily small rf magnetic field as long as one could vary the frequency slowly enough to conserve entropy but still fast enough so that T_1 processes would not be important.

Continuous Wave Line Shape

If a small linearly polarized rf magnetic field $H_1 \cos\omega t$ is applied along the x axis, then the steady-state magnetization in the x direction is given by

$$M_x = H_1[\chi'(\omega)\cos\omega t + \chi''(\omega)\sin\omega t], \tag{74}$$

where the susceptibilities are given by[7]

$$\chi'(\omega) = -\frac{i}{\hbar}\int_0^\infty \cos\omega t \,\mathrm{Tr}\left\{\left[\rho_0, \exp\left(-\frac{i}{\hbar}\mathcal{H}t\right)M_x\right.\right. \times\left.\left.\exp\left(\frac{i}{\hbar}\mathcal{H}t\right)\right]M_x\right\}dt, \tag{75}$$

$$\chi''(\omega) = -\frac{i}{\hbar}\int_0^\infty \sin\omega t \,\mathrm{Tr}\left\{\left[\rho_0, \exp\left(-\frac{i}{\hbar}\mathcal{H}t\right)M_x\right.\right. \times\left.\left.\exp\left(\frac{i}{\hbar}\mathcal{H}t\right)\right]M_x\right\}dt, \tag{76}$$

where $M_x=\gamma\hbar\sum_n I_{xn}{}^a$. The ordinary cw resonance line shape is calculated by substituting Eq. (56) for ρ_0 to yield, after expanding the exponentials and substituting in Eq. (76),

$$\chi_N''(\omega) = \frac{i}{\hbar\alpha kT}\int_0^\infty \sin\omega t \,\mathrm{Tr}\left\{\left[\mathcal{H}, \exp\left(-i\frac{\mathcal{H}}{\hbar}t\right)M_x\right.\right. \times\left.\left.\exp\left(i\frac{\mathcal{H}}{\hbar}t\right)\right]M_x\right\}dt. \tag{77}$$

Using the fact that

$$\frac{d}{dt}\mathrm{Tr}\left\{\exp\left(-\frac{i}{\hbar}\mathcal{H}t\right)M_x\exp\left(\frac{i}{\hbar}\mathcal{H}t\right)M_x\right\} = -\frac{i}{\hbar}\mathrm{Tr}\left[\mathcal{H}, \exp\left(-\frac{i}{\hbar}\mathcal{H}t\right)M_x\exp\left(\frac{i}{\hbar}\mathcal{H}t\right)\right]M_x, \tag{78}$$

and integrating by parts, we find

$$\chi_N''(\omega) = \frac{\omega}{\alpha kT}\int_0^\infty \cos\omega t \,\mathrm{Tr}\left\{\exp\left(-\frac{i}{\hbar}\mathcal{H}t\right)M_x \times\exp\left(\frac{i}{\hbar}\mathcal{H}t\right)M_x\right\}dt. \tag{79}$$

Since nonsecular terms are neglected, we can write

$$\exp\left(-\frac{i}{\hbar}\mathcal{H}t\right) = \exp\left(-\frac{i}{\hbar}\mathcal{H}_0t\right)\exp\left(-\frac{i}{\hbar}\mathcal{H}_2t\right), \tag{80}$$

and use the term $\exp[-(i/\hbar)\mathcal{H}_0t]$ as a simple rotation operator to obtain, after simplification, the normal cw line shape:

$$\chi_N''(\omega) = \frac{\omega}{2\alpha kT}\int_0^\infty \cos(\omega-\Omega)t \,\mathrm{Tr}\{M_x^*(t)M_x\}dt, \tag{81}$$

where

$$M_x^*(t)M_x = \exp[-(i/\hbar)\mathcal{H}_2t]M_x\exp[(i/\hbar)\mathcal{H}_2t]M_x.$$

In order to calculate the cw line shape after ADRF, we use Eq. (68) for ρ_0. On expanding the exponential, ρ_0 becomes

$$\rho_0 = (1/\alpha)(1-\mathcal{H}_2/kT), \tag{82}$$

which can be rewritten as

$$\rho_0 = \frac{1}{\alpha}\left(1-\frac{\mathcal{H}_0+\mathcal{H}_2}{kT}+\frac{\mathcal{H}_0}{kT}\right). \tag{83}$$

Since the constant unity does not enter into the calculation, it is seen that to the first order in $1/kT$

$$\exp(-\mathcal{H}_2/kT) = \exp[-(\mathcal{H}_0+\mathcal{H}_2)/kT] - \exp(-\mathcal{H}_0/kT). \tag{84}$$

As Eq. (76) is linear in ρ_0, and χ'' has been calculated for $\rho_0=\exp(-\mathcal{H}/kT)$, it suffices to calculate χ'' for $\rho_0=\exp(-\mathcal{H}_0/kT)$ and combine the two results to obtain χ'' for $\rho_0=\exp(-\mathcal{H}_2/kt)$. This procedure is adopted since it results in simplifying the calculation. Using the notation of the qualitative section, we find

$$\chi_D'' = \chi_N'' - \chi_Z''. \tag{85}$$

Substituting $\rho_0=-\mathcal{H}_0/kT$ into Eq. (76) yields

$$\chi_Z''(\omega) = \frac{i}{\alpha kT\hbar}\int_0^\infty \sin\omega t \,\mathrm{Tr}\left\{\left[\mathcal{H}_0, \exp\left(-\frac{i}{\hbar}\mathcal{H}t\right)M_x\right.\right. \times\left.\left.\exp\left(\frac{i}{\hbar}\mathcal{H}t\right)\right]M_x\right\}dt, \tag{86}$$

which can be simplified by noting that since $[\mathcal{H}_0,\mathcal{H}]=0$, the exponential terms can be taken outside the commu-

tator and then, using

$$[\mathcal{H}_0, M_x] = i\hbar H_0 M_y \gamma, \tag{87}$$

we obtain

$$\chi_Z''(\omega) = -\frac{\Omega}{\alpha k T}\int_0^\infty \sin\omega t \,\mathrm{Tr}\left[\exp\left(\frac{i}{\hbar}\mathcal{H}t\right)M_x \times \exp\left(-\frac{i}{\hbar}\mathcal{H}t\right)M_y\right]dt. \tag{88}$$

In a similar manner to that used in obtaining Eq. (81), we find

$$\chi_Z''(\omega) = \frac{\Omega}{2\alpha k T}\int_0^\infty \cos(\omega-\Omega)t \,\mathrm{Tr}[M_x^*(t)M_x]dt, \tag{89}$$

so that, using Eq. (85), we obtain the desired expression for $\chi_D''(\omega)$:

$$\chi_D''(\omega) = +\frac{(\omega-\Omega)}{2\alpha k T}\int_0^\infty \cos(\omega-\Omega_0)t \times \mathrm{Tr}[M_x^*(t)M_x]dt. \tag{90}$$

The expressions for $\chi_N'(\omega)$, $\chi_Z'(\omega)$, $\chi_D'(\omega)$ are obtained in a similar manner. We find

$$\chi_N'(\omega) = -\frac{\omega}{2\alpha k T}\int_0^\infty [\sin(\omega-\Omega)t+\sin(\omega+\Omega)t] \times \mathrm{Tr}(M_x^*(t)M_x)dt - \left(\frac{1}{\alpha k T}\right)\mathrm{Tr}M_x^2;$$

$$\chi_Z'(\omega) = -\frac{\Omega}{2\alpha k T}\int_0^\infty [\sin(\omega-\Omega)t - \sin(\omega+\Omega)t]\,\mathrm{Tr}(M_x^*(t)M_x)dt; \tag{91}$$

$$\chi_D'(\omega) = -\frac{(\omega-\Omega)}{2\alpha k T}\int_0^\infty \sin(\omega-\Omega)t\,\mathrm{Tr}(M_x^*(t)M_x)dt - \frac{(\omega+\Omega)}{2\alpha k T}\int_0^\infty \sin(\omega+\Omega)t\,\mathrm{Tr}(M_x^*(t)M_x)dt + \left(\frac{1}{\alpha k T}\right)\mathrm{Tr}M_x^2.$$

The above expressions for $\chi'(\omega)$ and $\chi''(\omega)$, although quite formal, are very useful. It should be noticed that all the above expressions are just Fourier transforms of the term $\mathrm{Tr}[M_x^*(t)M_x]$. Since the power absorbed from an rf field is $A(\omega)=2\omega\chi''H_1^2$, we may use Eqs. (8) and (81) to obtain

$$G(\omega) = \frac{1}{\pi\,\mathrm{Tr}M_x^2}\int_0^\infty \cos(\omega-\Omega)t\,\mathrm{Tr}[M_x^*(t)M_x]dt. \tag{92}$$

On inverting, we obtain

$$\mathrm{Tr}[M_x^*(t)M_x] = 2\,\mathrm{Tr}M_x^2\int_0^\infty G(\omega'+\Omega)\cos\omega' t d\omega'. \tag{93}$$

We write the susceptibilities in more concise form:

$$\begin{aligned}
&\chi_N''(\omega) = \omega G(\omega);\\
&\chi_Z''(\omega) = \Omega G(\omega);\\
&\chi_D''(\omega) = (\omega-\Omega)G(\omega);\\
&\chi_N'(\omega) = \omega[F_-(\omega)+F_+(\omega)]+F_0;\\
&\chi_Z'(\omega) = \Omega[F_-(\omega)-F_+(\omega)];\\
&\chi_D'(\omega) = (\omega-\Omega)F_-(\omega)+(\omega+\Omega)F_+(\omega)+F_0,
\end{aligned} \tag{94}$$

where

$$F_0 = \chi_0,$$

$$F_-(\omega) = \frac{-\chi_0}{2\,\mathrm{Tr}M_x^2}\int_0^\infty \sin(\omega-\Omega)t\,\mathrm{Tr}\{M_x^*(t)M_x\}dt, \tag{95}$$

$$F_+(\omega) = \frac{-\chi_0}{2\,\mathrm{Tr}M_x^2}\int_0^\infty \sin(\omega+\Omega)t\,\mathrm{Tr}\{M_x^*(t)M_x\}dt.$$

The above susceptibilities are all determined once $g(\omega)$ is known. As an illustrative example consider $g(\omega)$ as the Gaussian function Eq. (21). Using this function $F_-(\omega)$ becomes

$$F_-(\omega) = -\frac{1}{\sqrt{2}}\chi_0 T_2 \exp\left[\frac{-(\omega-\Omega)^2T_2^2}{2}\right] \times \int_0^{[(\omega-\Omega)T_2/\sqrt{2}]} \exp(t^2)dt \tag{96}$$

and

$$F_+(\omega,\Omega) = F_-(\omega,-\Omega). \tag{97}$$

The susceptibilities $\chi_Z''(\omega)$, $\chi_D''(\omega)$, $\chi_Z'(\omega)$, and $\chi_D'(\omega)$ were numerically evaluated over the range $-2\leq(\omega-\Omega)T_2/\sqrt{2}\leq 2$ and plotted in Fig. 2. In this Gaussian approximation it is readily noticed that

$$\chi_D''(\omega) \simeq (1/\Omega T_2^2)(d/d\omega)\chi_Z''(\omega), \tag{98}$$

and

$$\chi_D'(\omega) = -(1/\Omega T_2^2)(d/d\omega)\chi_Z'(\omega). \tag{99}$$

The fact that Eq. (98) is satisfied for a Gaussian line could have been stated in the qualitative section after Eq. (10) was obtained. The result indicated by Eq. (99) then follows by a simple application of the Kramers-Kronig relationship.

Free-Induction Decay

We consider the effect of applying a short intense rf pulse to the spin system. If a θ^0 rf pulse is applied to a spin system in thermal equilibrium with the lattice, ρ_0 being given by Eq. (56), then a free-induction decay

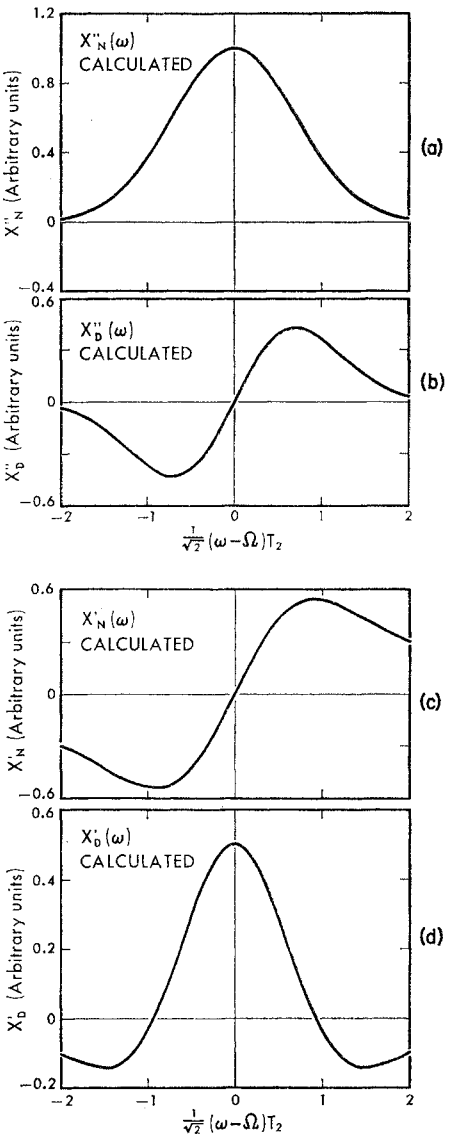

FIG. 2. Theoretical curves are given for χ'' and χ' before and after ADRF over the range $-2\leq(\omega-\Omega)T_2/\sqrt{2}\leq 2$. The subscript N signifies the normal NMR case (before ADRF); the subscript D signifies the case after ADRF.

signal will be observed whose envelope is given by[13]

$$\langle M_x\rangle_Z=\gamma^2\hbar^2H_0\sum_{n,m}\mathrm{Tr}\{I_{xm}{}^a\exp[-(i/\hbar)\mathcal{H}_2 t]\times(I_{xn}{}^a/\alpha kT)\exp[(i/\hbar)\mathcal{H}_2 t]\}\sin\theta. \quad (100)$$

It is easily verified that this expression is just the Fourier transform of the line shape given by Eq. (81).

Consider next a θ^0 rf pulse being applied to the above set of spins after ADRF when ρ_0 is given by Eq. (68). Proceeding in the same manner in which Eq. (100) was obtained, we obtain a free-induction signal envelope given by

$$\langle M_x\rangle_D=(\gamma\hbar/\alpha kT_S)\sum_{ijn}\mathrm{Tr}\{I_{xn}\exp[-(i/\hbar)\mathcal{H}_2 t]\times[B_{ij}(I_{z_i}{}^aI_{y_i}{}^a+I_{y_i}{}^aI_{z_j}{}^a)\cos\theta+C_{ij}I_{y_i}{}^aI_{z_j}{}^b]\times\exp[(i/\hbar)\mathcal{H}_2 t]\}\sin\theta. \quad (101)$$

Note that at $t=0$, $\langle M_x\rangle_D=0$, but that the derivative of $\langle M_x\rangle_D$

$$d\langle M_x\rangle_D/dt\,|_{t=0}=(M_0/\langle\Delta\omega_L{}^2\rangle^{1/2})[\langle\Delta\omega_{aa}{}^2\rangle\cos\theta+\langle\Delta\omega_{aa}{}^2\rangle]\sin\theta, \quad (102)$$

is not, in general, equal to zero. Equation (67) was used to eliminate T_S in the above equation. This expression suggests a method for determining the ratio of $\langle\Delta\omega_{aa}{}^2\rangle/\langle\Delta\omega_{ab}{}^2\rangle$ directly by simply noting $d\langle M_x\rangle_D/dt$ at $t=0$ as a function of θ.

It is interesting to note that Eq. (101) is not the Fourier transform of the corresponding line shape Eq. (90). The Fourier transform of Eq. (90) is given by

$$F(\chi_N'')=K(d/dt)\,\mathrm{Tr}[M_x{}^*(t)M_x], \quad (103)$$

where K is a constant factor. $F(\chi_N'')$ can be rewritten as

$$F(\chi_N'')=K\sum_{ijn}\mathrm{Tr}\{I_{xn}\exp(-i\hbar\mathcal{H}_2{}^*t)[B_{ij}(I_{z_i}{}^aI_{y_j}{}^a+I_{y_i}{}^aI_{z_j}{}^a)+C_{ij}I_{y_i}{}^aI_{z_j}{}^b]\exp[(i/\hbar)\mathcal{H}_2{}^*t]\}. \quad (104)$$

On comparing Eqs. (101) and (104), it is seen that Eq. (104) is the Fourier transform of the line shape only in the special case of either B or C being equal to zero, that is to say, the line must be either completely homogeneously or inhomogeneously broadened and not some mixture of both. In the limit that $B\gg C$

$$\langle M_x\rangle_D=(1/\langle\Delta\omega_L{}^2\rangle^{1/2})(d/dt)\langle M_x\rangle_Z\cos\theta, \quad (105)$$

and when $C\gg B$

$$\langle M_x\rangle_D=(1/\langle\Delta\omega_L{}^2\rangle^{1/2})(d/dt)\langle M_x\rangle_Z, \quad (106)$$

while, in general, $\langle M_x\rangle_D$ is given by either

$$\langle M_x\rangle_D=(1/\langle\Delta\omega_L{}^2\rangle^{1/2})(d/dt)\langle M_x\rangle_Z\cos\theta+(\gamma\hbar/\alpha kT_S)\sum_{nij}\mathrm{Tr}\{I_{xn}\exp[-(i/\hbar)\mathcal{H}_2 t]\times C_{ij}I_{y_i}{}^aI_{z_j}{}^a\exp[(i/\hbar)\mathcal{H}_2 t](1-\cos\theta)\}\sin\theta, \quad (107)$$

or

$$\langle M_x\rangle_D=(1/\langle\Delta\omega_L{}^2\rangle^{1/2})(d/dt)\langle M_x\rangle_Z-(\gamma\hbar/\alpha kT_S)\sum_{nij}\mathrm{Tr}\{I_{xn}\exp[-(i/\hbar)\mathcal{H}_2 t)B_{ij}(I_{z_i}I_{y_j}+I_{y_i}I_{z_j})\exp[(i/\hbar)\mathcal{H}_2 t)]\}(1-\cos\theta)\sin\theta. \quad (108)$$

If the resonance line is Gaussian, then the normal free-induction decay described by Eq. (100) is given by

$$\langle M_x\rangle_Z=M_0\exp(-t^2/2T_2{}^2)\sin\theta, \quad (109)$$

and the slope of the signal envelope is given by

$$d\langle M_x\rangle_Z/dt=(M_0t/T_2^2)\exp(-t^2/2T_2^2)\sin\theta. \quad (110)$$

In order for Eqs. (110) and (100) to be compatible, it is necessary that

$$-\sum_{ijn}(\gamma^2\hbar H/\alpha kT)\,\mathrm{Tr}\{I_{xn}{}^a\exp[-(i/\hbar)\mathcal{H}_2t]\times B_{ij}(I_{zi}{}^aI_{yj}{}^a+I_{yi}{}^aI_{zj}{}^a)\exp[(i/\hbar)\mathcal{H}_2t]\}=(M_0t/T_{2aa}{}^2)\exp(-t^2/2T_2^2), \quad (111)$$

and

$$-\sum_{ijn}(\gamma^2\hbar H/\alpha kT)\{I_{xn}{}^a\exp[-(i/\hbar)\mathcal{H}_2t]\times C_{ij}I_{yi}{}^aI_{zj}{}^a\exp[(i/\hbar)\mathcal{H}_2t]\}=(M_0t/T_{2ab}{}^2)\exp(-t^2/2T_2^2), \quad (112)$$

where $1/T_2{}^2=(1/T_{2aa}{}^2)+(1/T_{2ab}{}^2)$, T_{2aa} refers to inverse second moment due to unprimed spins only, and T_{2ab} refers to contribution of the second moment of the unprimed spins due to the primed spins.

Upon evaluation of the trace expressions in Eqs. (111) and (112) to first and second order, it is found that the equations are satisfied. Equations (111) and (112) will break down when higher order corrections are made. Let us now use the approximate expressions given in Eqs. (111) and (112) to evaluate $\langle M_x\rangle_D$ in Eq. (101). We obtain

$$\langle M_x\rangle_D=\frac{1}{\langle\Delta\omega_L{}^2\rangle^{1/2}}\frac{d\langle M_x\rangle_Z}{dt}\left[\frac{\langle\Delta\omega_{aa}{}^2\rangle\cos\theta+\langle\Delta\omega_{ab}{}^2\rangle}{\langle\Delta\omega_{aa}{}^2\rangle+\langle\Delta\omega_{ab}{}^2\rangle}\right], \quad (113)$$

which is equivalent to Eq. (46), obtained using purely heuristic arguments.

CW Line Shape after Prolonged Irradiation

If a homogeneously broadened line is irradiated after ADRF, a change in line shape occurs. The resulting line shape appears to be arising from a spin system which has both Zeeman and dipole-dipole energy. The following discussion is an attempt to explain the above phenomenon.

Consider the general case in which the density matrix is given by

$$\rho_0=(1/\alpha)\exp[-(\mathcal{H}_0{}^a/kT_Z)-(\mathcal{H}_2/kT_D)], \quad (114)$$

where T_Z is the temperature of the Zeeman system and T_D is the temperature of the dipole-dipole system. If a small rf magnetic field [satisfying Eq. (73)] is applied, then in the rotating frame the Zeeman and dipole-dipole systems will be coupled and a common spin temperature will be attained. The assumption is that immediately after the application of the rf magnetic field, the density matrix in the rotating frame ρ^* is given by

$$\rho^*=(1/\alpha)\exp\{-[(\Omega_a-\omega)/\Omega_a](\mathcal{H}_0{}^a/kT_Z{}^*)\}\times\exp(-\mathcal{H}_2/kT_D{}^*), \quad (115)$$

and when equilibrium has set in

$$\rho^*=\frac{1}{\alpha}\exp\left(\frac{-[(\Omega_a-\omega)/\Omega_a]\mathcal{H}_0{}^a-\mathcal{H}_2}{T_S{}^*}\right). \quad (116)$$

Since the rf field is very small, it may be treated as a small perturbation which couples the two systems. With this assumption, the energy in the rotating frame

$$\mathcal{E}=\frac{1}{\alpha}\mathrm{Tr}\left[\left(\frac{(\Omega_a-\omega)}{\Omega_a}\mathcal{H}_0{}^a+\mathcal{H}_2\right)\rho^*\right], \quad (117)$$

is a constant of the motion and $T_S{}^*$ may be calculated on the basis of conservation of energy. On this basis

$$T_S{}^*=\frac{(\Omega_a-\omega)^2\,\mathrm{Tr}\mathcal{H}_0{}^{a2}+\Omega_a{}^2\,\mathrm{Tr}\mathcal{H}_2{}^2}{(\Omega_a-\omega)^2\,\mathrm{Tr}\mathcal{H}_0{}^{a2}T_D{}^*+\Omega_a{}^2\,\mathrm{Tr}\mathcal{H}_2{}^2T_Z{}^*}T_D{}^*T_Z{}^*. \quad (118)$$

The effect of turning the rf field on or off does not change the entropy of the system, so that

$$T_D=T_D{}^*, \quad (119)$$

and

$$T_Z{}^*=[(\Omega_a-\omega)/\Omega_a]T_Z. \quad (120)$$

When a common spin temperature has been reached (assume T_1 is infinite) the rf field is turned off and the density matrix takes the form of Eq. (114) with $T_Z\rightarrow T_{Zf}$ and $T_D\rightarrow T_{Df}$, where

$$T_{Zf}=[\Omega_a/(\Omega_a-\omega)]T_S{}^*, \quad (121)$$

and

$$T_{Df}=T_S{}^*. \quad (122)$$

Since $\mathrm{Tr}|\mathcal{H}_0{}^a|^2/\mathrm{Tr}\mathcal{H}_2{}^2=\Omega^2/\omega_L{}^2$, we may write

$$T_{Zf}=\frac{\Omega_a}{\Omega_a-\omega}\left(\frac{(\Omega_a-\omega)^2+\omega_L{}^2}{\Omega_a(\Omega_a-\omega)T_D+\omega_L{}^2T_Z}\right)T_DT_Z,$$

and (123)

$$T_{Df}=\left(\frac{(\Omega_a-\omega)^2+\omega_L{}^2}{\Omega_a(\Omega_a-\omega)T_D+\omega_L{}^2T_Z}\right)T_DT_Z.$$

The ratio T_{Zf}/T_{Df} is given by

$$T_{Zf}/T_{Df}=\Omega_a/(\Omega_a-\omega), \quad (124)$$

which is independent of the initial temperatures. Since the line shape depends only on the ratio the above result clearly shows that after prolonged irradiation the line shape will, in general, be quite different than before irradiation and in particular (i.e., for times of order T_1) the normal homogeneously broadened Zeeman line may become permanently distorted by this process. Only in the case where $\omega=\Omega$ is the Zeeman line saturated uniformly. Another result following from the above equations is that the line after prolonged irradiation at ω is independent of the line shape before irradiation. Only the magnitude of the resonance line depends on the original line shape. In the case when

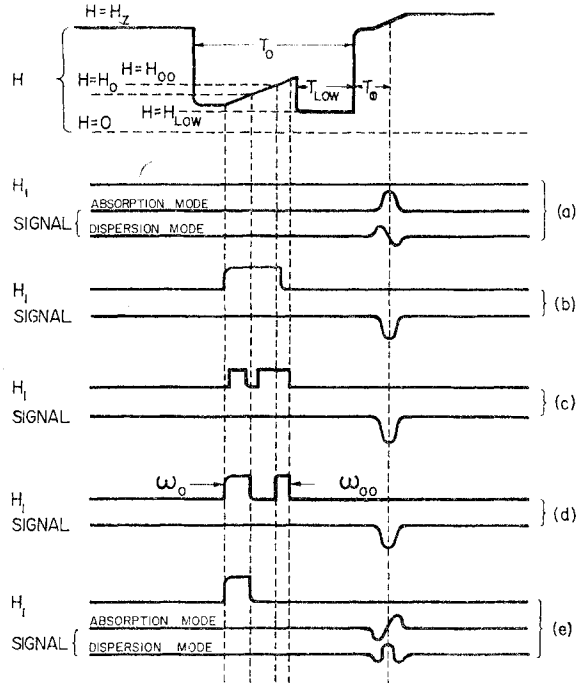

FIG. 3. This experiment is performed at fields H_0 (and H_{low}) and the system changes are observed at fields H_z. Typically, the fields H_z are of order 700 G and the fields H_0 are of order 50 G. Time T_0 is short compared with the spin-lattice relaxation time, T_1. The experiments are described in the text; 3(a), for example, has a normal absorption signal which is seen at high field following adiabatic variations of the dc field to and from H_0. The system observed is Li^7 in lithium metal.

the line is also inhomogeneously broadened, the above results only apply when the rf can be applied for a time short compared to T_1 but long enough for the spin system to be described by a single spin temperature in the rotating frame. This situation might be difficult to achieve in practice.

Another interesting result follows from Eq. (123), namely, that if the spin system is initially at equilibrium with the lattice, i.e., $T_Z=T_D=T$, $\omega>\Omega$, and $|\Omega-\omega|<\omega_L^2/\Omega$, then it follows that T_{Zf} is negative. This indicates that it is possible to invert the resonance line by simply irradiating slightly off and above resonance; in the cases considered here (Li^7 metal and NaCl) this effect would be masked by the dipole-dipole contribution to line shape.[14]

Experimental Method

Both cw and pulse techniques have been used in the study reported here. The cw method is shown in Fig. 3 and is described in more detail elsewhere.[15] In this method the system (in this case a lithium metal dispersion with particle size small enough to neglect rf skin effect) is polarized at high dc field for times long compared with T_1. The dc field is then adiabatically lowered to fields below H_0, following which a sweep is made through field H_0. After the sweep the system is left at field H_{low} (for a period, T_0), where the effects of other rf fields or relaxation phenomena can occur. At the conclusion of the period T_0 the dc field is adiabatically returned to high field and observations are made of line shape and amplitude on a passage through the high-field resonance line. The use of high dc fields for developing a polarization and high frequencies for observation brings considerable sensitivity to this method, while the performance of experiments at lower dc fields may be handled so long as the spin-lattice relaxation time, T_1, is long compared with the time, T_0, at low field. The high-field rf is weak in the sense that it does not produce substantial saturation (or inversion) on the passage through resonance while the low-field rf is generally high in this sense. The frequency of observation at high field was 1.1 Mc/sec and the temperature was about 1.3°K; T_1 for this case is about 35 sec. The variable dc fields are provided by a relay-gated air core solenoid. Observed signals at high field are obtained by use of 270-cycle dc field modulation and lock-in techniques with a crossed coil rf head. Low-frequency rf fields were provided by use of relay gating of these rf voltages to the normal high-frequency transmitter or modulation coils. Typical low-field H_1 values were of order 0.2 G. Dc sweep fields were provided by transistor driven sweeps.

The method used for pulse technique observations is shown in Fig. 3. In this case it was possible to apply intense rf pulses of variable time durations to observe free induction decay signals and spin echoes. The rf amplifier was so designed that a 90° phase shift could be introduced in the rf magnetic field and the rf amplitude could be controlled electronically to produce either slow (adiabatic) or rapid (nonadiabatic) H_1 variations. Water doped with Fe^{3+} or Na nuclei in a single crystal of NaCl were used in these experiments.

Experimental Results and Discussion

A number of experiments will now be discussed with reference to Figs. 1 and 3. These experiments show in some detail the interesting properties of spin systems which have been adiabatically demagnetized in the rotating frame, ADRF.

Figure 1(a) shows the normal signal which is obtained when no low-field H_1 is applied. The signals illustrate the normal absorption and dispersion signals characteristic of the Li^7 spin system in lithium metal. In Fig. 3(b), the H_1 field is applied during the passage through the low-field resonance and the magnetization is inverted during this passage; the inverted signal is consequently seen at high field. The rf, H_1, was sufficiently high to produce 90% inversion. Neither case 3(a)

[14] The possibility of inverting a line by the application of a small rf field applied off resonance has also been communicated to the authors by H. Reich (private communication).

[15] A. G. Anderson and A. G. Redfield, Phys. Rev. **116**, 583 (1959).

nor 3(b) represent new material, but rather illustrate the experimental method. In these cases, and most others reported here as well, the naturally occurring Li^6 in the lithium sample has no significant effect on the results observed because of its small concentration and the small nuclear moment of Li^6.

Demagnetization and Remagnetization in the Rotating Frame

Following the experiments of Redfield[3] and more recent work of Slichter and Holton[2] on studies of the magnetization in the rotating reference frame, it is of interest to extend that work to the case where the rf field, H_1, is reduced to zero; that is, to consider an experiment where the magnetization in a dipole-dipole broadened spin system is first aligned along H_{er}, the effective field in a frame rotating at the rf frequency, ω, and where H_{er} is subsequently decreased to zero. If the variation of H_{er} occurs slowly enough that the process is truly adiabatic, then the entropy or order is conserved and alignment along H_{er} is replaced by alignment within dipole-dipole fields. Such a variation, of course, changes the relative values of Zeeman and dipole-dipole energy in the spin system and one must consider the coupling between Zeeman and dipole-dipole energies to determine the stability of such a change. So long as the dc magnetic field is high enough that, in the absence of H_1, the coupling time, T_{12} (for transfer from dipole-dipole energy to Zeeman energy), is very long compared with T_1, then the change should be stable and reversible if performed in times short compared with T_1. If T_{12} were short then, after demagnetization, equilibrium between dipole-dipole energy and Zeeman energy would be reached in a short time with a final Zeeman energy much reduced from the initial Zeeman energy before demagnetization. There is a considerable body of experimental evidence, some of it included in this paper, which indicates that, for dc fields of order 10 times the local fields, T_{12} values of greater than seconds can be expected in nuclear spin systems.

In a demonstration of ADRF reversibility several experiments were performed. In the first of these, using Li^7 in lithium metal, Fig. 3(c), the rf was shut off for time durations of the order of 50 msec. This period represents a small fraction of the total time necessary to sweep through resonance, so that with the turn-off and turn-on symmetrical about the line center, it is a good approximation to view this rf gating as occurring at resonance. After the H_1 field was so turned off and on at resonance during the sweep through the line, the subsequently inverted signal amplitude was observed at high field. The signal so observed was equal, within 10%, in amplitude to the signal observed when H_1 was left on continuously throughout the fast passage; further, the small decrease in signal observed is dependent upon the H_1 turn-off time in a manner quite

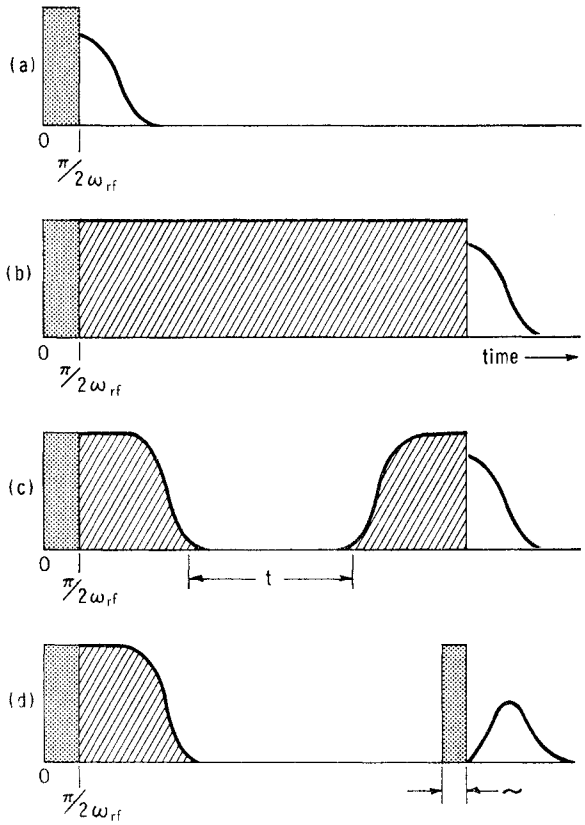

FIG. 4. Pulse experimental method. The shaded portion represents the applied rf field. The discontinuity in the shading represents a 90° phase discontinuity in the applied rf field. The unshaded portion represents the amplitude of the resulting free induction decay. (a) A normal free induction decay resulting from a 90° pulse. (b) A "spin locked" free-induction decay signal resulting from the magnetization which was polarized along the applied rf field. (c) The rf field is turned off and on slowly to perform an ADRF experiment. (d) A free-induction decay caused by a pulse after ADRF.

consistent with the signal loss to be expected from the fact that the dc field actually changes during this rf off-on interval.

As mentioned previously, the H_1 fields used in Fig. 3 are of order 0.2 G. The work of Slichter and Holton shows the reversibility of the demagnetization process down to fields of this order as does the inversion experiment in Fig. 3(b) since the effective field in the rotating frame goes from a large positive value—to H_1—to a large negative value during the sweep. The gating at the line center extends the experiment down to H_1 (and H_{er}) equal zero.

In the second experiment to examine this reversibility, using the method of Fig. 4, the Na^{23} magnetization in NaCl was first aligned along H_1 in the rotating frame and then H_1 was slowly lowered to zero and then slowly raised to its former value. For this case $(H_1)_{max}$ was of order of $\langle \Delta H \rangle_{av}$. The magnetization obtained along H_1 following this sequence was measured by decreasing H_1 nonadiabatically (short time com-

pared to T_2) to zero and observing the free induction decay. In this experiment which combines adiabatic variation of H_1 and nonadiabatic variation of H_1 (for readout) it was found that with the crystal oriented with the magnetic field along the 110 direction one recovers the initial magnetization to within 10% while with the magnetic field along the 100 direction the recovery was within 20%.

Demagnetization in the Rotating Frame at ω_0 and Remagnetization at ω_{00}

It was a straightforward extension of the previous experiments to consider a case where the rf, H_1, was left off for times longer than the time required to sweep through the low field line, Fig. 3(d). In this case it was readily found (again with Li^7 in lithium) that if H_1 is decreased to zero at ω_0, i.e., at resonance for the field H_0, then the full value of the magnetization is re-established by subsequently raising H_1 at frequency ω_{00} and completing the sweep. The frequency ω_{00} is equal to γH_{00}, where H_{00} is the value of the field at the time of reapplication of the rf. Reapplication of H_1 at frequencies other than ω_{00} produced a loss of magnetization and a change of observed signal shape (see below).

This experiment demonstrates the fact that the system has a well-defined "resonance" frequency, even in the demagnetized state where energy is in dipole-dipole alignment and where the system energy is, at fields large compared to $\langle \Delta H \rangle_{av}$, independent of dc field. This is to be expected since after ADRF the energy is all in the dipole-dipole system and in order to adiabatically remagnetize, it is necessary to apply an effective field in the rotating frame which increases slowly from a zero value. This is only possible if the frequency of the applied rf is at resonance with the nuclear spins, this frequency not being necessarily the frequency at which demagnetization occurs.

Observation of the Demagnetized System—CW Method

One of the most interesting experiments performed by the method of Fig. 3 was that illustrated in Fig. 3(e), the observation of the "resonance" line at high field after adiabatic demagnetization in the rotating frame, ADRF. Figure 1 shows a comparison of high-field line shapes obtained in several experimental cases, in good agreement with the theoretical curves of Fig. 2. These experimental lines were obtained by integration of the experimental signals shown in Fig. 5. The high-field method of observation used in this experiment included 270-cycle dc field modulation and lock-in detection to obtain the derivative curves of Fig. 5, with subsequent manual integration to obtain the lines of Figs. 1 and 3. A comparison between direct receiver output signals (without field modulation) and the integrated lock-in output indicated that no unusual effects were occurring

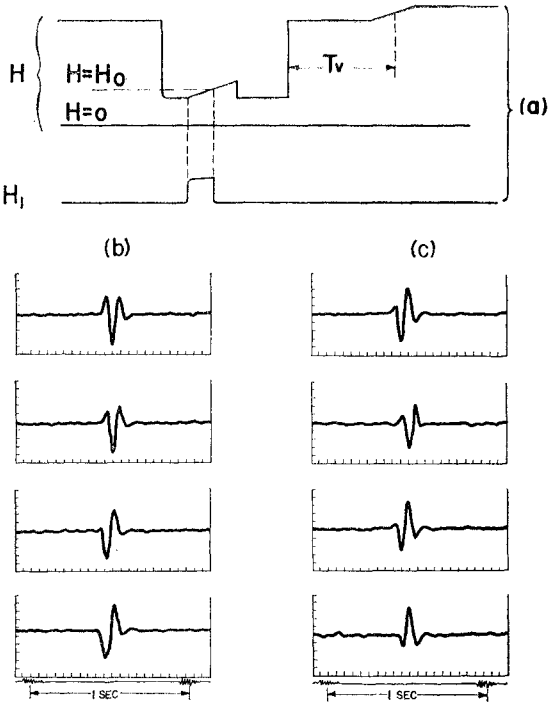

FIG. 5. The variation with time of the observed signals at high field. (a) The method is shown at the top of the figure, where adiabatic demagnetization is produced at low field and the relaxation from the demagnetized state to the normal high-field state takes place at high field. Signals shown are obtained by lock-in techniques and are derivatives of the true lines. (b) Absorption mode showing the demagnetized signal and the change with time as the normal absorption mode signal grows. The last signal shown must be multiplied by a factor of 2 for a recording scale change, while the first signal shown is that obtaining by low-field ADRF. (c) Dispersion mode signal change with time as the normal dispersion grows from the initial ADRF state.

in the latter method. A comparison of Figs. 1, 3, and 5 shows the markedly different absorption and dispersion mode signals obtained in the normal and the ADRF cases.

The normal absorption mode signal has the familiar shape (Fig. 1) symmetrical about the line center (neglecting the experimental "bump" on the right which is believed to be a bridge balance effect). On the other hand, the ADRF absorption line is decidedly nonsymmetrical and has, in fact, odd symmetry about the line center. Equation (94) predicts this latter line shape for the case where the spin system has order only in internal alignment.

The dispersion mode signals in Fig. 5(c) show a significant change in the ADRF state for this mode also. The ADRF dispersion signal appears as definitely a derivative (with respect to frequency) of the normal signal and is well described by Eq. (98).

The relative amplitudes of the signals obtained in both normal and ADRF cases have been discussed in previous sections. As pointed out there, and as seen in Fig. 1, these signals have comparable amplitudes even though the spin system energy in the normal case is a

factor of (H_z/H_L) greater, after taking into account the reduced spin temperature of the dipole-dipole system after ADRF.

Negative and Positive Temperatures in ADRF

While in the experiment illustrated in Fig. 3(e) the dc field starts below H_0 and sweeps up through it, one could equally well consider the case where the field starts above H_0 and sweeps down through H_0. In the latter case the magnetization begins aligned *along* the effective field in the rotating frame and in the process of ADRF one obtains a low *positive* temperature in the dipole-dipole system. In the former case, the magnetization is initially aligned *opposite* to the effective field and after ADRF a *negative* temperature is obtained in the dipole-dipole systems. The two cases are and have been readily distinguished experimentally by a difference in sign of the observed signals; a similar case in normal adiabatic demagnetization is implicit in the experiments of Ramsey and Pound.[16]

Observation of ADRF-Pulse Methods

The types of signals observed above suggested the phenomenological (inhomogeneous) model discussed in the introduction, with a zero total magnetization and part of the magnetization along the positive z axis and part of the magnetization along the negative z axis with a separation in center frequencies for the positive and negative parts. This suggests a pulse experiment where, following ADRF, a 90° pulse is applied to the system. Signals to be expected are predicted by Eq. (46), with an initial zero signal which rises to a peak in the time, of order T_2, required for the positive and negative parts of the magnetization to precess from destructive into constructive interference. Equation (101), which originates from the more detailed theory, predicts similar behavior.

In order to experimentally demonstrate some of these effects in an inhomogeneously broadened system, a 90° pulse followed by a 180° pulse was applied to a sample containing water doped with Fe^{3+} ions. Figure 6 shows the experimental results obtained for the 90° to 180° sequence applied to both a normal and an ADRF system. The photographs show clearly that Eq. (46) gives a good description of the experimental results following the 90° pulse. On the basis of that discussion one expects that the ADRF echo at $t=2\tau$, where τ is the 90° to 180° separation time, the spins would again be oppositely directed to yield zero signal, as is also shown in Fig. 6; the echo is not antisymmetric in this figure because phase sensitive detection was *not* used.

The case in which there is homogeneous (as well as inhomogeneous) broadening of the line is of considerable interest since from Eq. (46) and the more precise Eq. (102) we expect that the initial slope of the free induction decay from a pulse after ADRF will vary with

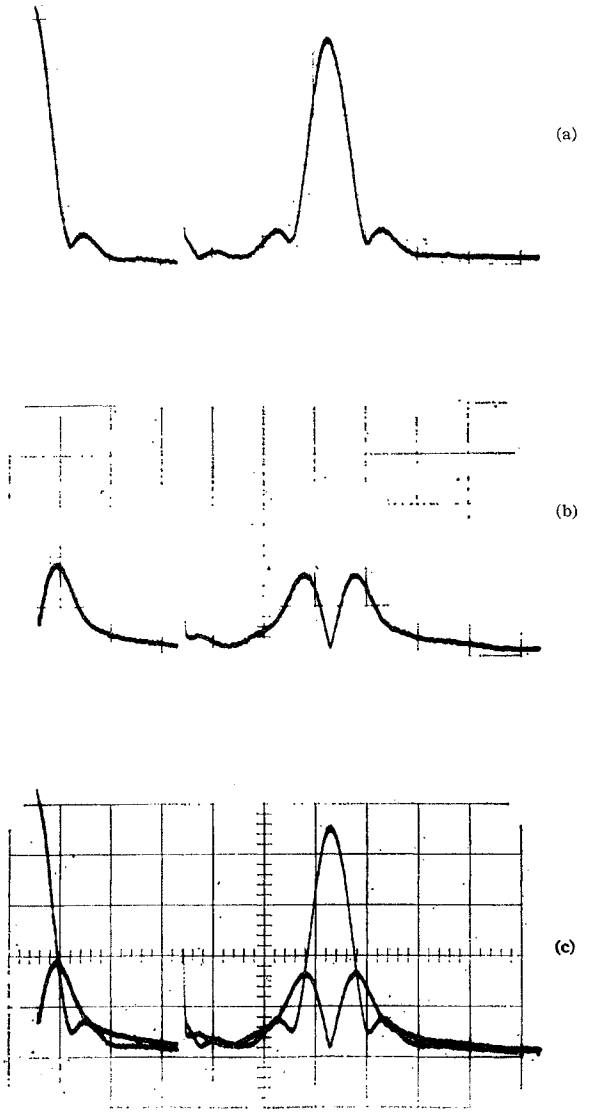

FIG. 6. Spin echo signals of protons in Fe^{3+}-doped water. The dc field was made inhomogeneous in order to sharpen the echo. (a) Normal spin echo; (b) spin echo after ADRF; (c) above signals superimposed.

pulse length in a manner determined by the second moments due to like and unlike spins. This latter more complicated behavior is a result of the changing of the local fields at the spin sites resulting from the application of the rf pulse. This effect can be illustrated clearly by observing the free induction decay of Na^{23} in NaCl after ADRF for H_0 in the [100] direction and also for H_0 in the [110] direction. The results are shown in Fig. 7 where the initial slope is plotted against rf pulse width. A theoretical curve is given in each case based on a numerical calculation of the second moments due to like and unlike nuclei, with 30 nearest Cl neighbors used in calculating $\langle\Delta\omega_{ab}^2\rangle$ and 38 Na neighbors used in calculating $\langle\Delta\omega_{aa}^2\rangle$. It was found that the

[16] N. F. Ramsey and R. V. Pound, Phys. Rev. 81, 278 (1951).

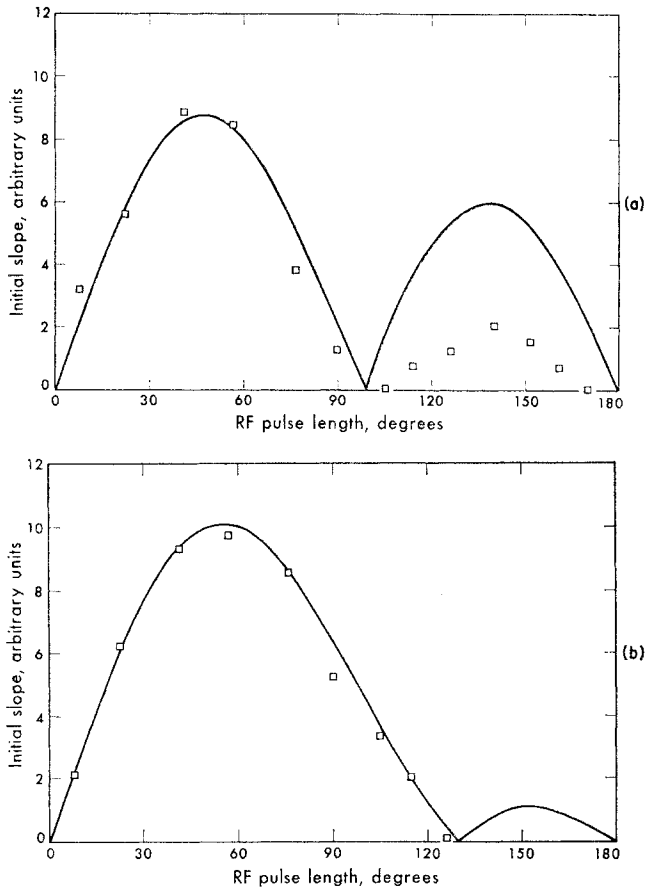

FIG. 7. Initial slope of free induction decay signal of Na in NaCl after adiabatic demagnetization. The solid line is a theoretical curve. The applied field is along the [100] direction for curve (a) and along the [110] direction for curve (b).

ratio $\langle\Delta\omega_{ab}^2\rangle/\langle\Delta\omega_{aa}^2\rangle$ was 0.644 in the [100] direction and 0.134 in the [110] direction.

Experimental difficulties were encountered in the slope measurements because the rf amplitude used was of the same order as ΔH; this produces, in addition to the expected free induction decay which should start at zero, a second free induction decay, originating in a residual magnetization, which is a maximum after the pulse and subsequently decays in the conventional manner. This second signal is a result of conversion of dipole-dipole alignment into alignment along the rf field. It was expected that by measuring the initial slope of the free induction decay after ADRF one would be able to measure the ratio $\langle\Delta\omega_{aa}^2\rangle/\langle\Delta\omega_{ab}^2\rangle$ very accurately: In order to achieve such accuracy, however, more intense and spatially uniform rf pulses will be required.

It is interesting to note that if an rf field is slowly applied to an inhomogeneously broadened line on resonance and then instantaneously shut off, a signal is obtained which is much like the signal obtained with a pulse after ADRF. This is so because part of the magnetization lines up along, and part lines up against, the applied rf in the rotating frame, a process considerably different from ADRF although yielding a similar type signal.

Time Dependence of High-Field Line Shape

Figure 5 shows another interesting feature of the observed lines which is obtained by extension of the method of Fig. 3. In this case, Fig. 5, a variable time delay, T_v, is introduced in place of the fixed time, T_d (Fig. 3) and the spin system is prepared at low field by the method of ADRF. The line observed at high field is then expected to vary with T_v, going from the shape of Fig. 3(e) at $T_v=T_d$ to the shape of Fig. 3(a) at $T_v\gg T_1$. Between these cases the absorption line shape is a linear supposition of the $g(\nu)$ and $[(\nu-\nu_0)/\nu]g(\nu)$ functions. The experimental signals in Fig. 5 show this variation of line shape for both modes of observation. The variation appears to be continuous and is indicative of a relaxation time in the adiabatically demagnetized state of about 10 to 15 sec while the normal spin lattice T_1 is about 35 sec for this Li^7 sample in lithium metal. Clearly, both the $g(\nu)$ and $[(\nu-\nu_0)/\nu]g(\nu)$ shapes are equilibrium shapes over times of this order, as are the dispersion and the derivative of the dispersion line shapes.

Saturation Dependence

It has also been found possible experimentally to apply rf power (Fig. 3, Li^7) to one or the other side of the demagnetized state absorption line during time interval T_{low} to partially saturate it at low field. The high-field line obtained in this manner is a residual line, indicating both $g(\nu)$ and $[(\nu-\nu_0)/\nu]g(\nu)$ contributions, which consists mainly of a normal absorption line or an inverted normal absorption line, dependent upon whether the low-field rf was applied to the low- or high-frequency part of the demagnetized line.

Interestingly enough, this behavior suggested another experiment in which the normal line was irradiated rather than the ADRF line. In this case, again using Li^7 in lithium metal, the normal line was subjected to an intense rf H_1 (but still small compared to $\langle\Delta H\rangle_{\text{av}}$) for several seconds at a frequency within the absorption spectrum. The resultant line shape was then, once again, observed at high field. Equations (123) and (124) predict that asymmetry should be obtained in the resultant high-field line shape when the frequency of the low-field rf differs from exact resonance. This is indeed the case, with rather pronounced asymmetries being observed; the asymmetrical line observed, in agreement with Eq. (123) appears to be relatively independent of the rf magnitude once a steady-state configuration is reached. The dispersion lines observed appear to consist of a combination of normal and ADRF contributions. At this writing, however, it has not been experimentally verified that these equations,

when used with Eq. (94), predict the proper quantitative behavior. Further experimental work is in progress to check this point.

Either of these two saturation experiments demonstrates experimentally that these systems do not saturate uniformly and that one must be cautious in assumptions relating to uniform saturation of homogeneously broadened lines. In fact, in many cases a sizable signal is obtained in situations where uniform saturation behavior would have reduced the signal to zero many times over; of course, the recent work of Holcomb *et al.*[3,17] has also shown such behavior but without the severe asymmetries noted here. The asymmetries produced are permanent (for a time of order T_1) after the rf is turned off.

The above results may lead one to question whether it is *ever* possible to observe the true line shape. The answer here appears to be that such is possible under either of two cases in systems having only Zeeman and dipole-dipole interactions; the first is the case where the rf amplitude is sufficiently low and T_1 is sufficiently short that no significant departures from Zeeman and dipole-dipole energy equilibrium can occur; this is probably reasonably well described by requiring that the usual saturation parameter $(\gamma^2H_1^2T_1T_2)$ be small, a case recently restudied by Goldburg.[4] The second case is the case where H_1 is sufficiently small and the internal equilibrium time, T_{12}, is sufficiently short that significant internal equilibrium departures do not occur; one can anticipate that, by extension, difficulties will not be encountered if $(\gamma^2H_1^2T_2T_{12})$ is small.[18] Further cases can be anticipated, where the normal line shape is observed, if the system has short internal dipole-dipole system relaxation times due to coupling with paramagnetic impurities or other nuclei with short T_1.

Field Dependence of Relaxation Time in the Demagnetized State

Most of the previous results could be explained with an inhomogeneously broadened NMR line. However, the case here, representative of homogeneously broadened lines, *is* considerably different as is shown by an experiment with Li^7 in lithium metal in which the field dependence of relaxation times was measured in the ADRF state. The relaxation phenomena which occurs when the system is prepared as in Fig. 3(e) and the dc field is then made comparable with $\langle\Delta H\rangle_{\text{av}}$ is one in which, if T_1 is quite large for both normal and demagnetized systems, total energy is conserved but the ratio of Zeeman to dipole-dipole energy changes. The subject of such relaxation has been discussed by a number of authors,[5] both experimentally and theoretically. At zero field one expects Zeeman and dipole-dipole energies to be tightly coupled with a relaxation time of order T_2, while at higher dc fields the coupling should decrease to give a $T_{12}(H)\sim T_2\exp(H^2/c\Delta H^2)$, where c is a constant of order one, assuming a Gaussian line shape in the Larmor resonance line.

In this experiment, Li^7 was demagnetized at 60 kc/sec followed by a reduction to field H_{low} for a time T_{low} and the relaxation time measured. Relaxation times of 3 sec at 20 G, 0.5 sec at 15 G, and less than 20 msec at 10 G were obtained, while the normal high-field T_1 is 35 sec. The signal during relaxation essentially decays toward zero since energy is conserved and H_{low} is large compared with H_L. This process is not reversible. At the time of this writing these measurements are crude and additional work is being done to extend them.

However, crude as these results are, they clearly demonstrate a *fast* field dependence of relaxation time and the nonreversibility of a slow variation of the dc field to and from zero field after the system has been demagnetized. This is a specific property of the dipole-dipole coupled system and will not be the case for inhomogeneously broadened systems except for pathological cases. The arrangement here for preparing a spin system with a large dipole-dipole energy and low Zeeman energy and for observing the demagnetized-system time dependences may provide one with a unique experimental tool for the study of the internal relaxation processes of a single-species spin system. This is particularly true at high field where these processes are expected to be weak; at low fields the method must be compared with low-frequency spin-absorption methods[6,18] and another time-dependent method starting from zero field.[19] At high field the ADRF state is far from equilibrium and changes of dipole-dipole energy are readily observed; these factors lead to high sensitivity for the method.

High-field (where T_{12} is expected to be long) relaxation times of the ADRF state were measured in Li^7 at 1.3°K at 40 G ($T_1=14$ sec) and at 700 G ($T_1=10$–15 sec). The normal spin-lattice relaxation time, T_1, is 35 sec, throughout this range of dc fields. By analogy with work on the field dependence of normal NMR spin lattice relaxation,[15] one anticipates that T_1 in the ADRF state should be dc field independent at these high dc fields and of the order of one-half the normal T_1. This appears to be the case.

Measurements were also made of T_1 in Na in NaCl and it was found that $T_1\approx4.5$ sec in the ADRF state which is less by more than a factor of 2 of the normal T_1 of 12 sec for NaCl.[20]

An additional experiment considered here and suggested independently by Strombotne depends upon conservation of the dipole-dipole energy in a rapid dc field variation; if the dc field is instantaneously de-

[17] D. F. Holcomb, B. Pedersen, and T. R. Sliker, Phys. Rev. **123**, 1951 (1961).
[18] A. G. Anderson, Phys. Rev. **115**, 863 (1959); **125**, 1517 (1962).
[19] R. L. Strombotne, thesis, University of California, 1962 (unpublished); Bull. Am. Phys. Soc. **6**, 508 (1961).
[20] E. G. Wikner, W. E. Blumberg, and E. L. Hahn, Phys. Rev. **118**, 631 (1960).

creased to zero following adiabatic demagnetization in the rotating frame, then conservation of dipole-dipole energy would be expected in the rapid variation, and also for subsequent intervals of time, to give the partial equivalent of a normal dc field adiabatic demagnetization. This hypothesis, at the time of this writing, has not been successfully tested experimentally.

Absorption at Frequencies Other Than the Larmor Frequency

In several respects this paper contains preliminary reports of work in progress; this is particularly true in the present case.

It is possible to experimentally measure the complete absorption spectrum of the ADRF demagnetized system by establishing a dc field, H_{low}, for a period of time, T_{low}, following the demagnetization in the rotating frame. During time T_{low}, an additional rf field is applied to the system and following T_{low} the effect of this rf is observed at high field (Fig. 3). By analogy with the normal system[10] one might expect to observe absorption at zero frequency (extending out to frequencies of order $[(\Delta\nu_0)^2]^{1/2}$ and indicative of absorption of energy in the dipole-dipole system, but without change of Zeeman energy), at the Larmor frequency, and at double the Larmor frequency in either parallel or perpendicular fields, i.e., rf and dc fields either parallel or perpendicular to each other.

Not all lines have been observed at this writing, but several points of experimental interest can be made:

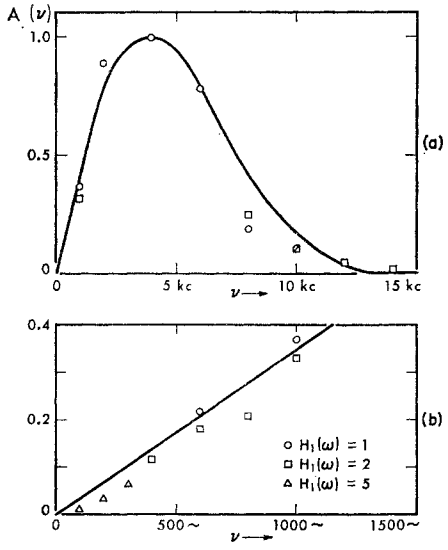

FIG. 8. Absorption, $A(\nu)$ [normalized to unit $H_1(\omega_1)$], at low frequencies after ADRF. The line shown is the equivalent of the "zero-frequency" line in the normal NMR case. In 8(a), the solid curve is given by $\nu\exp[\nu^2/2\langle\nu_0^2\rangle]$, where $\langle\nu_0^2\rangle$ is equal to 16 (kc/sec)^2 and gives a reasonable fit to the data, although there is no theoretical justification for its use at this time. In 8(b) the low-frequency data are compared with a linear frequency variation of absorption. The $H_1(\omega)$ are given in relative units and show a reasonably linear power dependence of absorption.

In the case of the low-frequency perpendicular line, shown in Fig. 8, the linewidth is of the same order as the normal Larmor linewidth. The energy absorbed per unit time is fairly well described by a distribution function, $\nu\exp(\nu^2/2\langle\Delta\nu_0\rangle^2)$, where ν is the applied frequency except for frequencies below several hundred cycles in which a ν^2 dependence appears to prevail. In agreement with Eq. (27b), the field dependence of total spin absorption in this line is approximately proportional to Ω^{-2} or H_0^{-2} (at 600 G as compared with the absorption at 40 G). The intensity is also in qualitative agreement with Eq. (27b).

Slight absorption of energy in the zero-frequency parallel-field case was observed. The power required to observe this absorption was orders of magnitude higher than that required for the perpendicular line, as would be expected from the equivalent normal case, and details of the spectrum were not recorded.

In the case of perpendicular-field second-harmonic absorption, the experimental line intensity is found to be lower than that for the zero-frequency perpendicular line and the line shape is similar to the Larmor frequency demagnetized line shape. Simple application of Eq. (34) would predict *larger* intensity for this comparison; however, when one makes the appropriate correction, Eq. (37b) for absorption in Zeeman and dipole-dipole systems, the shape and intensity appear reasonable. It is worth noting that application of rf at the second harmonic line results in production of a Zeeman component while rf at low frequency saturates the ADRF states uniformly as expected in the theoretical discussion.

It appears clear that more experimental and theoretical work is required to completely resolve the implications of these spectra.

Detection of Li^6 in Li^7

In the normal demagnetized state, i.e., at zero dc field, it is well known that two spin systems reach equilibrium rapidly by energy-conserving spin flips of the form $\uparrow\downarrow \rightarrow \downarrow\uparrow$ which bring both systems to a common spin temperature. It is natural enough to inquire if this is not likely to be the case also in multiple spin systems, one of which has undergone adiabatic demagnetization in the rotating frame. Considering a system with two spin species and using the phenomenological model with part of the magnetization along the positive z axis and part along the negative z axis (separated in field by $\sim\langle\Delta H\rangle_{\text{av}}$), one sees that such an arrangement in system 1 can be transferred to system 2 with conservation of energy; what is required is a $+-$ flip-flop in system 1 accompanied by a $-+$ change in system 2, a four-spin process. The arguments applied for cross relaxation processes[21] of other types could be applied here as well.

[21] N. Bloembergen, S. Shapiro, P. S. Pershan, and J. O. Artman, Phys. Rev. **114**, 445 (1959).

In an attempt to examine this problem, a lithium metal dispersion, enriched to 25% Li^6, was used in an experiment where rf was applied at the Li^6 resonance frequency, while examining the Li^7 signal at high field by the method of Fig. 3. It was found, as expected, that Li^7 in the normal state was insensitive to application of rf at the Li^6 frequency with or without z-axis modulation. It was also found that the Li^7 signal in the adiabatically demagnetized state was insensitive to the application of rf at the Li^6 frequency when *no z-axis* modulation was applied; what happens here is that Li^6 polarizes along the applied rf in its rotating frame and no energy is absorbed. Lastly, the Li^7 signal in the adiabatically demagnetized state *was* sensitive to the combination of rf at the Li^6 frequency *and* z-axis modulation and by this means the presence of Li^6 was readily observed; what happens in this case is that "rotary saturation"[3] takes place, i.e., absorption of energy in the Li^6 rotating frame from the z-axis modulation, and because of the Li^6–Li^7 coupling in the demagnetized state, the Li^7 system is saturated. Maximum rf H_1 fields at the Li^6 frequency were of order 0.2 G and z-axis modulation fields were of order 0.1 to 1.0 G.

The last experiment demonstrates the expected coupling between spin systems in the demagnetized state[22]; i.e., although for coupling of Zeeman energy there may be a prohibited interchange of spin populations, because of lack of conservation of energy in the interchange, there is no such prohibition in the case where the system energy is dipolar. Such interchanges may, in fact, have been responsible for some of the rather strange line shapes observed in double resonance experiments in the past.[23]

[22] E. L. Hahn and A. G. Redfield have independently arrived at similar conclusions (private communication).

IV. CONCLUSIONS

The experiments described above demonstrate a number of properties of spin systems connected with ADRF, the adiabatic demagnetization in the rotating frame. It is, in fact, shown that these processes can be reversible. Spectra of rather unusual form have been shown and explained for some of these pulse and cw experiments. The dipole-dipole system is well isolated from the Zeeman system at high fields and spin temperature concepts appear to be applicable.

ACKNOWLEDGMENTS

The authors would like to express their appreciation to Professor E. L. Hahn for interesting discussions, encouragement, and the use of his laboratory for the pulse work reported here, to Dr. L. S. Brown and Dr. J. M. Winter for interesting discussions, to H. Reich for review and comments, to C. Gabriel for a careful and critical review of the manuscript, and to H. Lee for assistance in the experimental work.

[23] Y. Masuda (private communication).